Precambrian Research 363 (2021) 106345

Contents lists available at ScienceDirect

Precambrian Research

journal homepage: www.elsevier.com/locate/precamres

Reassessing classic evidence for warm-based Cryogenian ice on the western Laurentian margin: The "striated pavement" of the Mineral Fork Formation, USA

T.M. Vandyk [a,*], C. Kettler [b], B.J. Davies [a], G.A. Shields [c], I. Candy [a], D.P. Le Heron [b]

[a] Department of Geography, Royal Holloway University of London, Surrey TW20 0EX, UK
[b] Department of Geology, University of Vienna, Althanstraße 14, A-1090 Vienna, Austria
[c] Department of Earth Sciences, University College London, Gower Street, London WC1E 6BT, UK

ARTICLE INFO

Keywords:
Cryogenian
Glaciation
Snowball Earth
Geomorphology

ABSTRACT

Determining the extent and nature of ancient glacial deposits is fundamental to understanding Earth's climate in the Cryogenian Period. Although the detailed study of sedimentary facies has allowed significant insights, it typically fails to produce high confidence interpretations for the past position of grounded ice, its thermal regime and flow direction, which are of fundamental importance to any glaciological reconstruction. When correctly identified, Cryogenian subglacially striated surfaces (pavements) unequivocally indicate grounded ice, a warm-based thermal regime and flow direction. However, they are globally rare and open to misinterpretation. Despite a discontinuous belt of Cryogenian strata, stretching thousands of kilometres from Alaska to California, the only purported Cryogenian pavements from the North American continent or the western margin of the Laurentian palaeocontinent occur in the Big Cottonwood Canyon area, Utah. We critically reappraise the only uncontested pavement from this area, presenting a detailed description derived from new high resolution photogrammetry and traditional field observations. These suggest that the purported pavement is unlikely to be a Cryogenian feature, but is instead a recent erosional phenomenon consistent with other structurally controlled features within the surrounding modern landscape. Our reinterpretation questions whether grounded Cryogenian ice reached the Utah – Idaho region and whether the lower reaches of the Mineral Fork Formation record glacially influenced deposition or non-glacial, rift-related sedimentation that transitions upwards into glacial conditions.

1. Introduction

During the Cryogenian Period (ca. 720–635 Ma) glaciation is hypothesised to have reached sea-level at equatorial latitudes, implying extreme global cold. However, our understanding of glacial dynamics and ice cover extent from this period remains poor (Kirschvink, 1992; Hoffman et al., 1998; Eyles and Januszczak, 2004; Abbot et al., 2011; Rose, 2015; Hoffman et al., 2017; Le Heron et al., 2020). Determining the past position of grounded ice, its thermal regime and flow direction are fundamental to improving that understanding. The study of sedimentary facies is rarely able to determine these three parameters with confidence as Cryogenian deposits tend to be the reworked products of glaciation, rather than directly deposited by grounded ice (Eyles and Januszczak, 2004; van Loon, 2008; Hambrey and Glasser, 2012; Spence et al., 2016). Subglacially striated bedrock surfaces (pavements) provide high-confidence evidence for grounded ice, a warm-based thermal regime and ice flow direction. They therefore have the potential to provide fundamentally important insights into Cryogenian glacial dynamics and ice cover extent, insights seldom possible through the study of sedimentary facies.

Cryogenian striated pavements are globally rare and known examples typically only exist as metre-scale fragments (Table 1). This is in unexplained contrast to pavements of the subsequent Late Palaeozoic Ice Age (LPIA), for example, that may be traced over hundreds of square kilometres (Trosdtorf et al., 2005; Le Heron, 2018; Assine et al., 2018; see Table 3 of Laajoki, 2002 for review of LPIA pavements). In addition to rarity, erroneous interpretation is a problem. Several of the few known Cryogenian striated pavements have alternatively been interpreted as non-glacial features (Table 1) (Daily et al., 1973; Christie-Blick, 1982; Jensen and Wulff-Pedersen, 1996). Given these challenges

* Corresponding author.
E-mail address: thomas.vandyk.2018@live.rhul.ac.uk (T.M. Vandyk).

https://doi.org/10.1016/j.precamres.2021.106345
Received 25 March 2021; Received in revised form 16 July 2021; Accepted 1 August 2021
Available online 17 August 2021

and the unique insights that pavements allow into Cryogenian ice dynamics and extent, the careful documentation and scrutiny of each and every example is essential.

On the North American continent, a discontinuous belt of Cryogenian glacigenic formations stretches thousands of kilometres, from Alaska to California, along the western margin of the Laurentian palaeocontinent (Fig. 1 A) (e.g. Macdonald et al., 2013; Yonkee et al., 2014; Moynihan et al., 2019). Despite this abundance of preserved strata, the only purported Cryogenian pavements known from the North American continent belong to the Big Cottonwood Canyon area of Utah (Fig. 1 B, C). These occur upon the Tonian (1000 Ma–ca. 720 Ma) Big Cottonwood Formation, immediately beneath the Cryogenian Mineral Fork Formation. They are reported in two modern day valleys, "Mill B North Fork" (Ojakangas and Matsch, 1980) and "Mill B South Fork" (Blick, 1979) (Fig. 1 C). Re-examination, however, has suggested that the purported Cryogenian pavements of Mill B South Fork are in fact a tectonic feature or the result of Pleistocene glaciation (Christie-Blick, 1982) (Supplementary Data). By contrast, no new data or scrutiny have been published from the purported pavement in Mill B North Fork since its initial description and interpretation over 40 years ago (Blick, 1979) (Fig. 2).

The purported Mill B North Fork pavement is therefore unique as the only uncontested Cryogenian pavement known on either the western Laurentian margin or the North American continent. If its subglacial interpretation is correct, it provides the highest confidence tie-point for grounded Cryogenian ice and ice flow direction on the western Laurentian margin. Increasing this potential significance, the Big Cottonwood Canyon area has not been significantly displaced by either the Sevier Orogeny or subsequent Basin and Range tectonics (Yonkee et al., 2014), which for the tectonically juxtaposed Cryogenian strata of the western Laurentian margin is almost unknown (Johnston, 2008) (Fig. 1 B).

Considering the potential importance of this purported pavement, advances in field techniques over the past 40 years and the interpretative difficulties associated with ancient pavements, reappraisal is long overdue. Our goal, therefore, is to critically reassess the purported Mill B North Fork pavement, presenting a detailed description derived from new high resolution photogrammetry and traditional field observations. These suggest that the purported pavement is unlikely to be a Cryogenian feature, but is instead a recent erosional phenomenon consistent with other structurally controlled features within the surrounding modern landscape.

1.1. Geologic Setting, age and previous work

1.1.1. Geologic setting

The Mineral Fork Formation of the Big Cottonwood Canyon study area is one of several Cryogenian glacigenic units in the Utah – Idaho region (Fanning and Link, 2004; Balgord et al., 2013; Keeley et al., 2013; Yonkee et al., 2014; Gaschnig et al., 2016) (Fig. 1 B). According to the regional reconstruction of Yonkee et al. (2014, their Fig. 12 A, B), these units were deposited in a north–south trending system of rift basins, accompanied by uplifted rift flanks. Subsequently, to the west of these glacigenic units, a passive margin developed during the Ediacaran to Cambrian periods (see $^{87}Sr/^{86}Sr$ isopleth in Fig. 1 A, B) (Armstrong et al., 1977; Elison et al., 1990). This margin then became active and accreted terranes from the Mesozoic onwards, inducing folding and thrusting during the Sevier Orogeny, followed by extensional "Basin and Range" tectonics (e.g. Yonkee and Weil, 2015).

As a consequence of this tectonic history, the Precambrian to Palaeozoic strata of the Big Cottonwood study area have been tilted towards the NE to NNE and form the northern limb of a gently eastward plunging anticline (e.g. Paulsen and Marshak, 1999) (Fig. 1 C). They were then rapidly exhumed between 10 and 5 million years ago (Armstrong et al., 2003). Whereas most of the Utah – Idaho region's Precambrian glacigenic units have been tectonically shifted eastward by 80 km to 150 km, the study area has been shifted only ~20 km and the neighbouring Provo area only ~50 km (compare "modern" and "restored" positions in Fig. 1 B) (Yonkee et al., 2014). During deposition of the Mineral Fork Formation, these two areas were further east and

Table 1
Neoproterozoic striated pavements.

Palaeocontinent (country)	Unit	Age	Discussion of age	Example of glacial/non-glacial interpretation	
				Glacial	Non-glacial
Baltica	Moelv Fm	E (?)	Nystuen and Lamminen (2011)	Nystuen and Lamminen (2011)	None
Central Iran	Kahar Fm	E	Etemad-Saeed et al. (2016)	Etemad-Saeed et al. (2016)	None
Rio de la Plata - Congo – São Francisco (Namibia)	Nama Grp	E	Germs and Gaucher (2012)	Germs (1972)	None
North Australia	Egan Fm	E	Grey and Corkeron (1998)	Corkeron (2011)	None
North China	Luoquan Fm	E	Le Heron et al. (2018)	Le Heron et al. (2018), Le Heron et al. (2019)	None
Morroco	Ouarzazate Grp	E	Vernhet et al. (2012)	Vernhet et al. (2012)	None
Baltica (Sweden)	Långmarkberg Fm	E (?)	Kumpulainen and Greiling (2011)	Asklund (1960)†	Crowell (1964)†
India	Blaini Fm	E/C (?)	Etienne et al. (2011)	Etienne et al. (2011)	Dey et al. (2020)
São Francisco (Brazil)	Jequitai Fm, Bebedouro Fm	C	de Andrade Caxito et al. (2012)	Isotta et al. (1969), Montes et al. (1985)	None
North Australia	Walsh, Fargoo, Landrigan Fm	C	Corkeron (2011)	Perry and Roberts (1968), Corkeron (2011)	None
Baltica (Norway)	Smalfjord Fm	C	Rice et al. (2011)	Rice and Hofmann (2000)	Jensen and Wulff-Pedersen (1996)
W. African Craton (Mauritania)	Jbéliat Grp	C	Deynoux (1985)	Shields-Zhou et al. (2011)	None
Laurentia (NE Greenland)	Tillite Grp	C	Stouge et al. (2011)	Moncrieff and Hambrey (1988)	None
Tarim (NW China)	Yuermeinak Fm	C	Vandyk et al. (2019)	Vandyk et al. (2019)	None
Laurentia (SW USA)	Mineral Fork Fm	C	This study	Blick (1979)	This study
South Australia	Merinjina Fm	C	Preiss et al. (2011)	Coats and Preiss (1987)	Daily et al. (1973)
East African Orogen (Oman)	Ayn Fm	C	Rieu et al. (2006)	Kellerhals and Matter (2003)	None

Note: E = Ediacaran, C = Cryogenian, Fm = Formation, Grp = Group. Certainty of age assignments is variable and the reader is directed to the references in the "Discussion of Age" column for further detail.
†as cited by Kumpulainen and Greiling (2011, p.626)

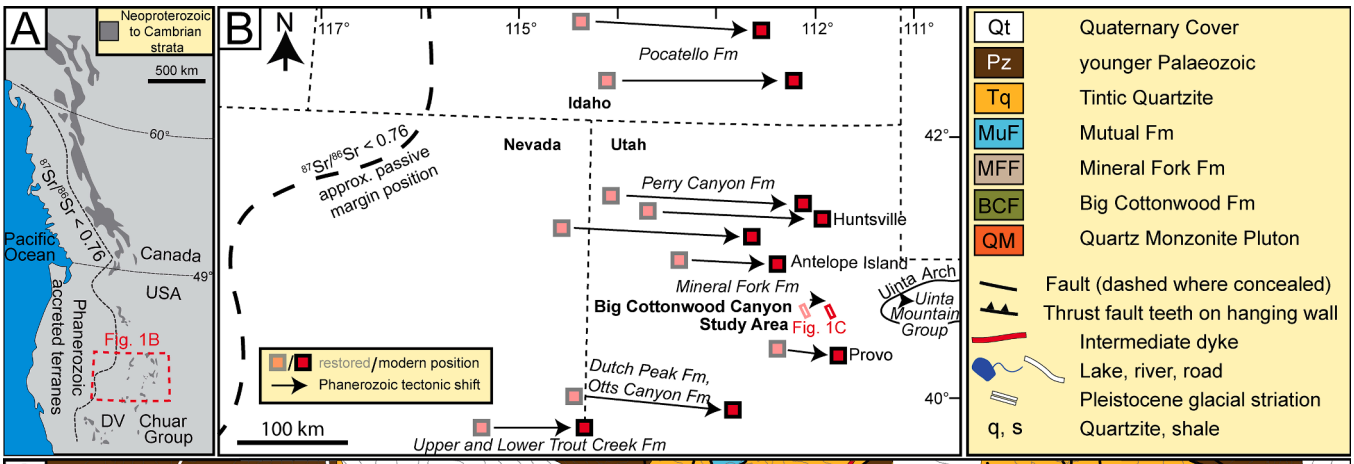

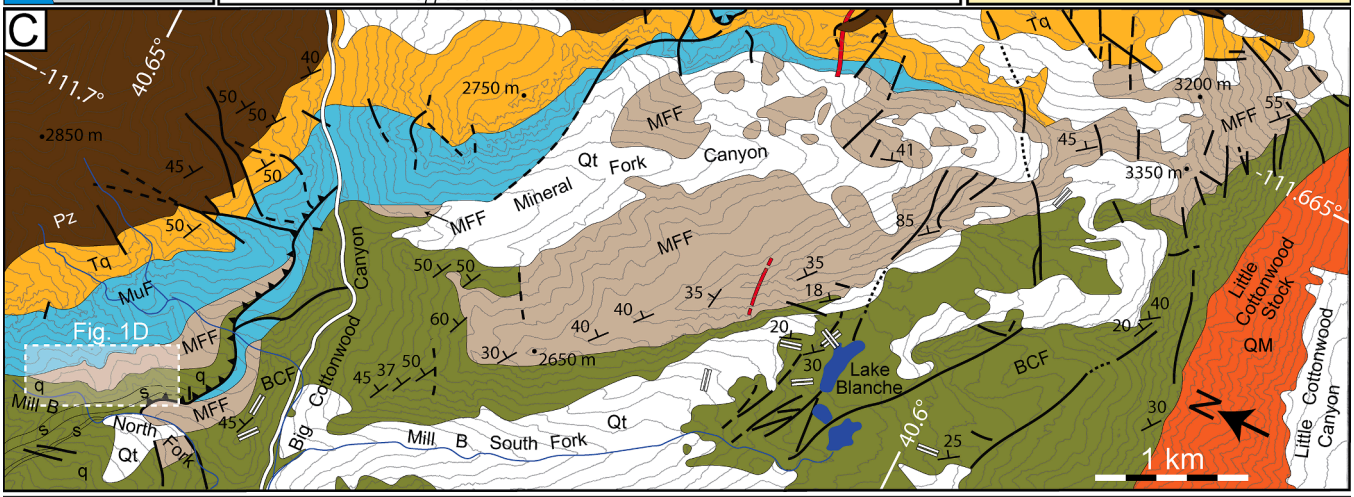

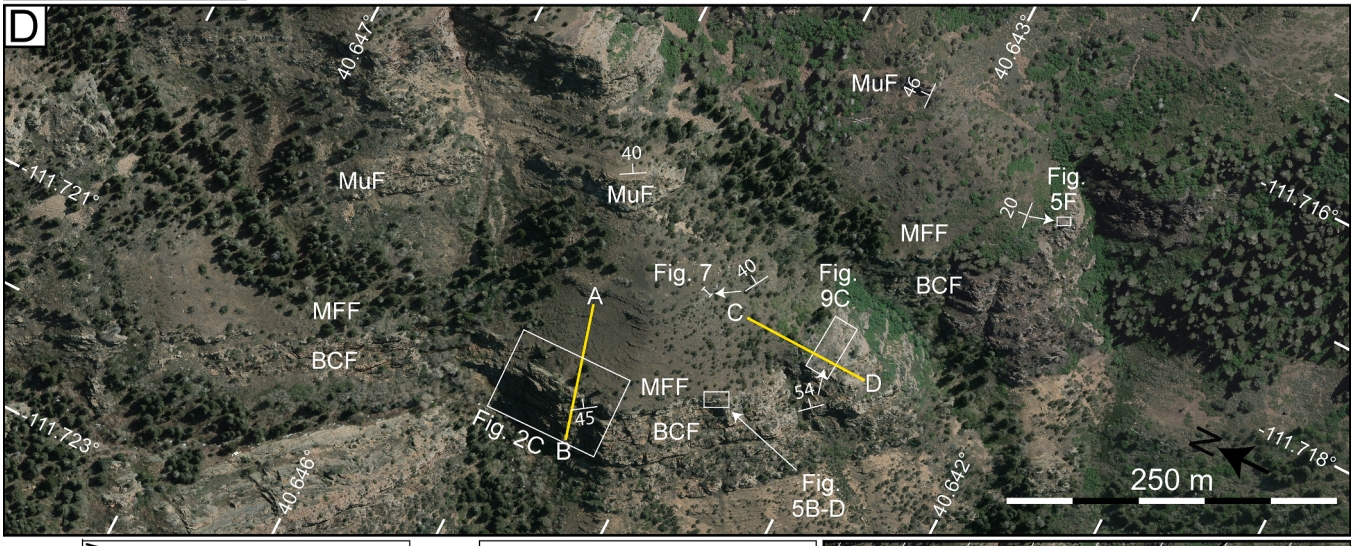

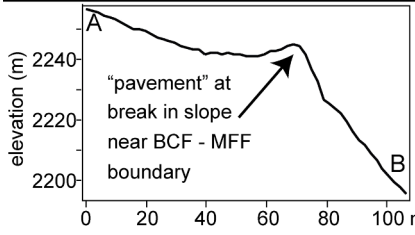

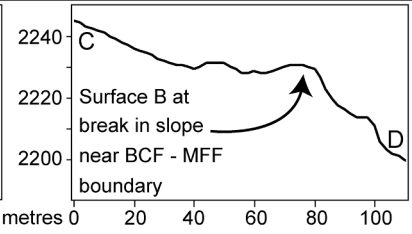

(caption on next page)

Fig. 1. Maps of study area. A: Western Laurentian Margin showing exposures of Neoproterozoic to Cambrian strata. DV: Death Valley. Modified from Fig. 1 of Yonkee et al. (2014). B: NW Utah – SE Idaho Region showing modern and restored positions of Cryogenian glacigenic units. Restored positions are position prior to Mesozoic to Cenozoic contractional (Sevier) then extensional (Basin and Range) tectonics. Ediacaran to Cambrian passive margin development occurred westward of the $^{87}Sr/^{86}Sr$ isopleth, which indicates the approximate western limit of Precambrian crystalline basement (Armstrong et al., 1977; Levy and Christie-Blick, 1989; Elison et al., 1990; Lund, 2008). Modified from Fig. 1 of Yonkee et al. (2014). Position given in Fig. 1A. C: Geologic map of study area, modified from Crittenden (1965a,b), Blick (1979 plate 4) and Christie-Blick (1983, Fig. 3). Contours derived from 2 m LIDAR (State of Utah, 2006). Unit boundaries slightly modified using 12.5 cm aerial photography (State of Utah, 2012) and ground observations. For clarity, the Big Cottonwood Formation has only been differentiated into quartzite (q) and shale (s) in Mill B North Fork. Position given in Fig. 1B. D: Orthomosaic of Mill B North Fork hanging wall with bedding orientation data of this study. 12.5 cm aerial photography (State of Utah, 2012). Positions of Fig. 2C (containing the "pavement"), Fig. 5B-D (fault grooves, ridge-in-groove, cataclastic material), Fig. 5E (partially abraded surface), Fig. 7 (Mineral fork Formation measured section) and Fig. 9C (Surface B) are indicated. Profile sections A-B and C-D demonstrate break in slope across the "pavement" (A-B) and Surface B (C-D) and are derived from 2 m bare Earth LIDAR (State of Utah, 2006). Subfigure at bottom right shows approximate position of unit boundaries. Position of D is given in Fig. 1C.

therefore closer to the rift flanks than any of the other Precambrian glacigenic units of the Utah – Idaho region (Fig. 12B, C of Yonkee et al., 2014).

The study area comprises Precambrian to Palaeozoic strata, partially obscured by Quaternary cover. Together, these form 4 valleys with intervening ridges: Mill B South Fork and Mineral Fork Canyon to the south of Big Cottonwood Canyon and Mill B North Fork to its north (Fig. 1 C). Mill B South Fork hosts a well-documented Pleistocene subglacially eroded landscape in its upper reaches, including streamlined and striated bedforms (Atwood, 1909; Quirk et al., 2018) (supplementary data). Contrastingly, no evidence of Pleistocene subglacial erosion has been reported from Mill B North Fork, which is sinuous, v-shaped and flanked by angular, joint-controlled cliffs. Minor faults of 100 m to km-scale length are common, predominantly striking E-W and NE-SW, as are similarly oriented dykes (Fig. 1 C). In Mill B North Fork, thrusting has duplicated the Precambrian strata. They are poorly exposed in a foot-wall block, which is not considered further, but better exposed in a hanging-wall block ~ 300 m to the N (Fig. 1 C, D). The purported Mill B North Fork pavement occurs upon this hanging-wall block (Figs. 1 D; 2).

From oldest to youngest, the Precambrian strata comprise the Big Cottonwood, Mineral Fork and Mutual formations. These are separated by sharp disconformable boundaries and are unconformably overlain by the Cambrian Tintic Quartzite (Fig. 1 C). The lower boundary of the Big Cottonwood Formation is not exposed. Its upper boundary has been deeply incised, prior to which strata were already consolidated (Link and Christie-Blick, 2011). The depth of this incision reaches ~180 m in Mill B North Fork and ~800 m in Mill B South Fork (Fig. 1 C). The incised boundary cannot be traced continuously between the two Forks (Fig. 1 C). According to the interpretation of Blick (1979), the purported pavement of Mill B North Fork occurs upon this incised upper boundary. Our observations, however, suggest that its stratigraphic position is less clear and that it may be stratigraphically lower than the formation boundary (see Section 3.1.1; Fig. 2 A-D).

Big Cottonwood Formation strata comprise slightly metamorphosed argillites to medium-grained rippled, cross-bedded or massive sandstones. Facies include tidal-fluvial and supratidal to shallow subtidal sedimentary rocks, within which tidal rhythmites confirm a marine connection (Ehlers and Chan, 1999). These were deposited at equatorial latitudes in an estuarine setting with westward-palaeoflows (Bressler, 1981; Ehlers and Chan, 1999; Weil et al., 2006).

The Mineral Fork Formation rests upon the incision into the top of Big Cottonwood Formation. It is overlain by the Mutual Formation or Palaeozoic strata (Fig. 1 C, D). In Mill B North Fork, it forms a ~2 km NW – SE elongate outcrop that reaches ~180 m thickness (Fig. 1 C, D). This pinches out to the NW and is truncated by a fault to the SE. Spanning Mill B South Fork to Mineral Fork Canyon, it forms a ~6 km NNW – SSE elongate outcrop that reaches ~800 m thickness. This is truncated by an inferred fault to the NNW and passes into multiple minor faults and non-exposure to the SSE (Fig. 1 C). The Mineral Fork Formation exposure therefore provides only a partial NW – SE or NNW – SSE section of exposure, which is too incomplete to allow confirmation of a U-shaped or any other glacially diagnostic valley geometry (c.f. Christie-Blick, 1983) (Fig. 1 C; see 3D model restored to palaeo-horizontal in Fig. S2 of the Supplementary Data). The upper boundary of the Mineral Fork Formation has been incised and its original thickness is therefore unknown (Condie, 1967; Ojakangas and Matsch, 1980; Levy et al., 1994).

The Mineral Fork Formation strata of the Big Cottonwood study area include laminated mudstones, massive to graded sandstones, clast-poor boulder-bearing diamictites and clast-supported cobble conglomerates (Crittenden et al., 1952; Condie, 1967; Varney, 1976; Blick, 1979; Ojakangas and Matsch, 1980; Christie-Blick, 1983). Cross-beds and ripples record water flowing towards the W to NNW and N respectively (Varney, 1976; Ojakangas and Matsch, 1980; Christie-Blick, 1983). A glacial influence during deposition of the Mineral Fork Formation has been suggested by most, but not all, authors (Hintze, 1914; Blackwelder, 1932; Varney, 1976; Ojakangas and Matsch, 1980; Christie-Blick, 1983). There is, however, no consensus regarding specific depositional processes or environments, other than general agreement that at least some of the strata were deposited by sediment gravity flows (i.e. turbidites or debrites) (Condie, 1967; Varney, 1976; Blick, 1979; Ojakangas and Matsch, 1980; Christie-Blick, 1983). Condie (1967) interpreted the strata entirely as sediment gravity flows but could not determine whether a glacial influence was present. They noted that the presence or absence of a striated pavement, which they searched for in vain, would be of particular importance in resolving this question (Condie, 1967 pp. 1320–1321).

Importantly, a "glacial influence" does not require grounded ice in the study area. Some Mineral Fork Formation diamictites have been interpreted as debrites (i.e. sediment gravity flows) and others as tillites (Condie, 1967; Varney, 1976; Ojakangas and Matsch, 1980; Christie-Blick, 1983). Tillites are deposited directly by glacial ice and not subsequently reworked by water, thus indicating the past presence of grounded ice. However, distinguishing between tillite and debrite in the ancient record remains problematic (e.g. Eyles and Januszczak, 2004; Arnaud and Etienne, 2011). In Mill B South Fork, Ojakangas and Matsch (1980) interpreted tillite from a long-axis bimodal clast orientation (e.g. Hicock et al., 1996) but subsequent research has suggested that tills cannot be reliably "fingerprinted" in this manner (e.g. Bennett et al., 1999; Benn and Evans, 2010; Hambrey and Glasser, 2012). Previous interpretations of tillite in the study area should therefore be treated as reasonable suggestions rather than high confidence interpretations.

1.1.2. Age of the Big Cottonwood and Mineral Fork formations

The youngest detrital zircons known from the Big Cottonwood Formation of the study area are around 1000 Ma (Dehler et al., 2010; Spencer et al., 2012; Yonkee et al., 2014). Five kilometres west of Mill B South Fork, Spencer et al. (2012) reported 4 zircons of 748 to 851 Ma from the Little Willow Formation. They correleated this formation with the Big Cottonwood Formation but considered their data unable to provide a precise maximum depositional age. Lithostratigraphic and palaeomagnetic correlations suggest that the Big Cottonwood Formation is a similar age to the Uinta Mountain Group, 50 to 220 km east of the study area (Fig. 1 B). This group has yielded a detrital zircon maximum depositional age of 766 ± 5 Ma (n = 4; 1σ) (Dehler et al., 2010). If palaeontologic and carbon isotopic correlations between the Uinta

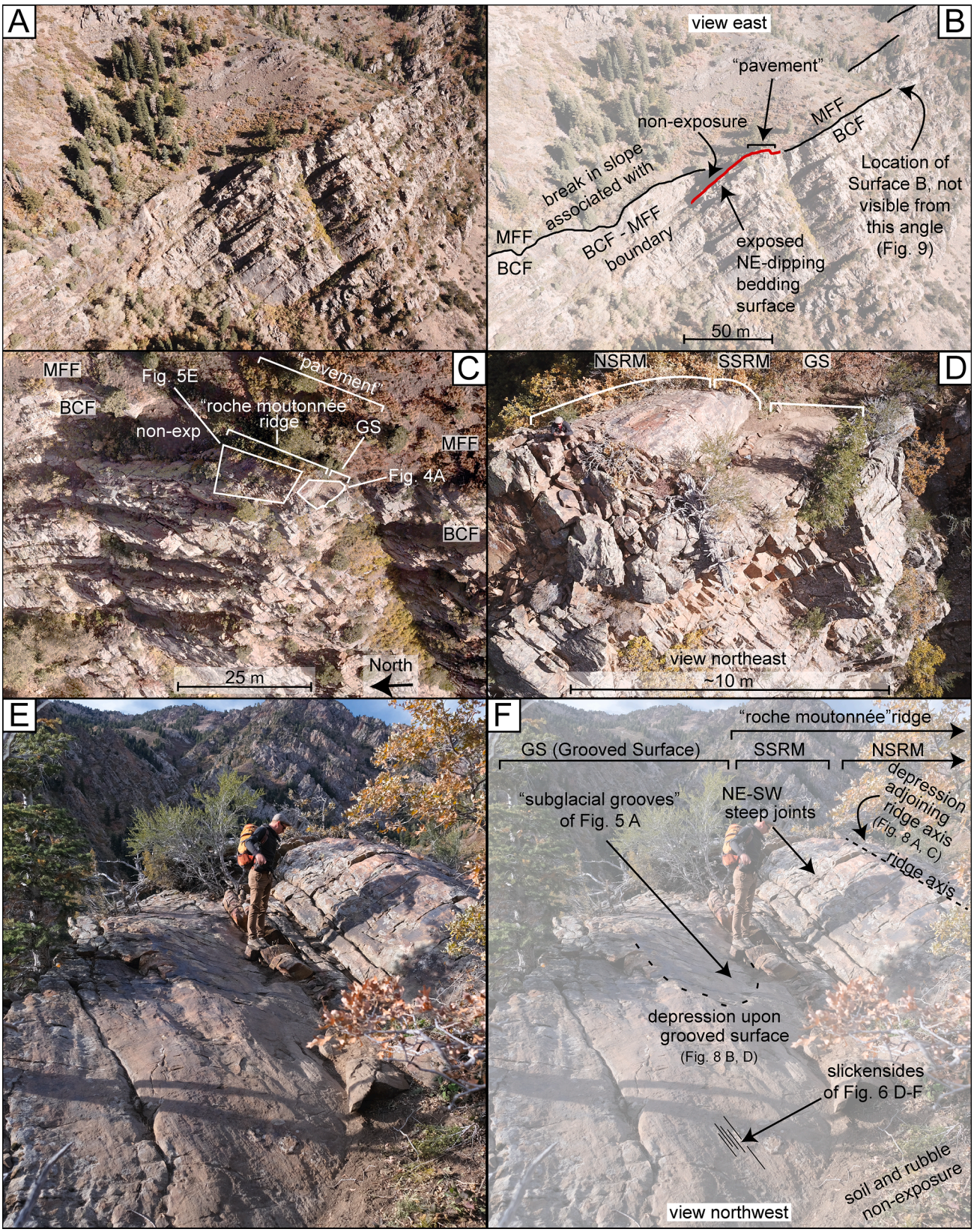

Fig. 2. The "pavement" in context. A, B: Location of "pavement" at the topographically highest end of a NE-dipping (056°/56°) Big Cottonwood Formation bedding surface. "non-exposure" is the same area as "non-exp" in Fig. 2 C. C: Vertical orthomosaic of the NE-dipping (056°/56°) Big Cottonwood Formation bedding surface. Built from 544 UAV images. Positions of Fig. 4A (high resolution orthomosaic of "pavement") and 5E (northern side of the "roche moutonnée" ridge) are indicated. "non-exp" is the same as non-exposure" in Fig. 2 B. D: Oblique UAV image of the "pavement". E, F: Oblique terrestrial image of the "pavement". Positions of Fig. 5A, 6D-F and 8 are indicated. Note that the full extent of the northern side of the "roche moutonnée ridge" is visible in Fig. 2C but not 2D-F. Abbreviations: NSRM-Northern Side of "Roche Moutonnée" Ridge; SSRM-Southern Side of "Roche Moutonnée" Ridge; BCF-Big Cottonwood Formation; MFF-Mineral Fork Formation.

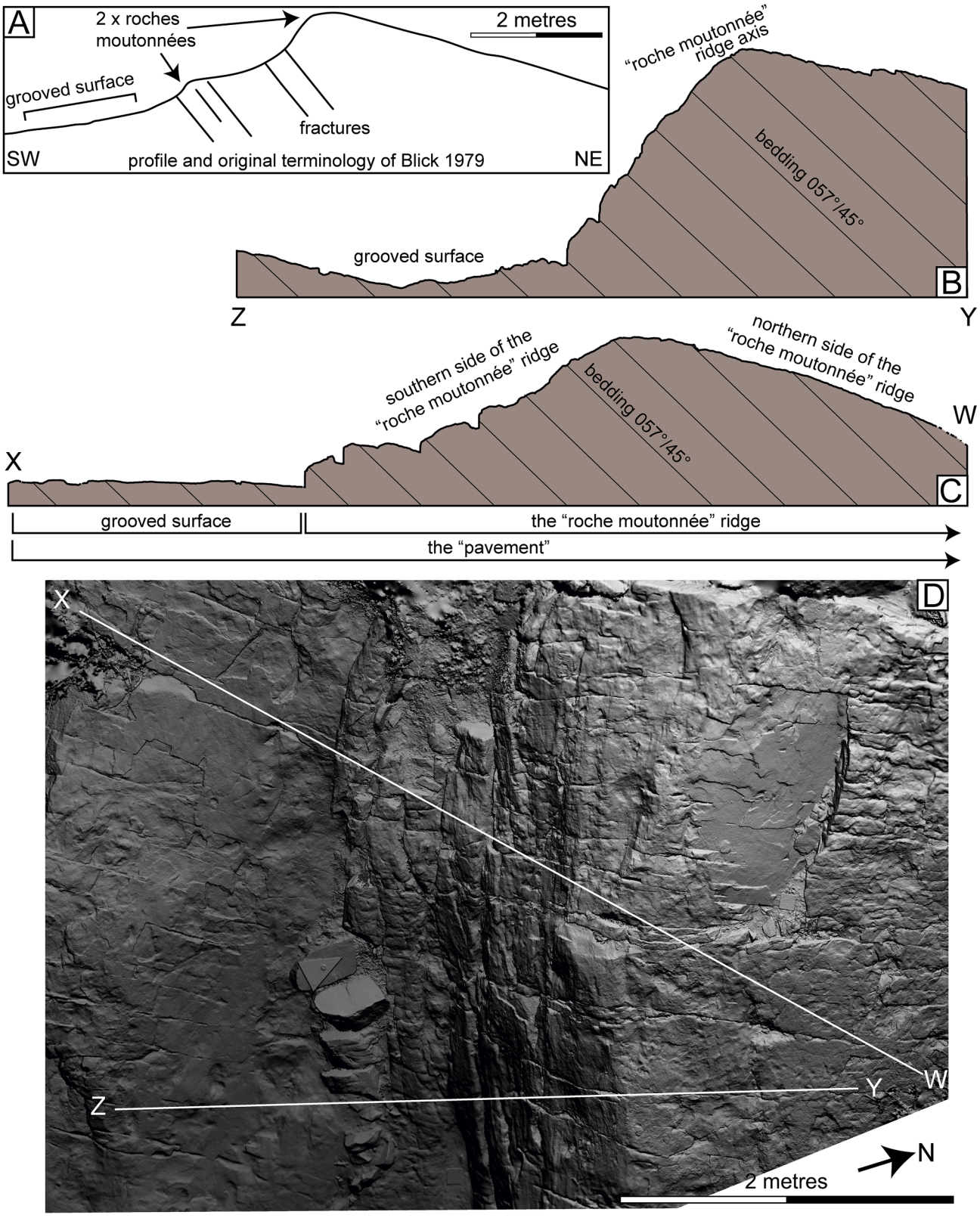

Fig. 3. A: Sketch profile and terminology minimally modified from Fig. 59 E of Blick (1979), showing his roche moutonnée ridges and grooved surface. B, C: Profiles WW-X and Y-Z across part of the northern side of the "roche moutonnée" ridge and onto the grooved surface, derived from digital elevation model (DEM) used in D. The positions of these profiles are shown in Fig. 3 D and Fig. 4 B as lines W-X and Y-Z D: Hillshade DEM. Position of profiles indicated. Source DEM built from 1039 terrestrial images, using the same point cloud as Fig. 4, with a nominal resolution of 0.48 mm/pix. Full resolution hillshade and source DEM available in Fig. S8 and DEM 1 of Supplementary Data.

Mountain Group and Chuar Group (Fig. 1 A) are correct, then a 742 ± 6 Ma ash layer in the latter places the tops of both groups around 740 Ma (Karlstrom et al., 2000; Dehler et al., 2010; Dehler et al., 2017).

The youngest detrital zircons extracted from the Mineral Fork Formation of the study area are ~1000 Ma (Yonkee et al., 2014). Two younger detrital zircons, 705 ± 41 Ma and 750 ± 16.5 Ma (1σ: Yonkee et al., 2014), have been extracted from the Mineral Fork Formation near Provo, today 45 km south of the study area (Fig. 1 B). The small number of these zircons, their high analytical uncertainty and an unclear stratigraphic relationship between the two areas suggest only a tentative maximum depositional age for the study area. Mudstones in the upper Mineral Fork Formation of the study area approach the composition of an iron formation ($Fe_2O_3t \leq 14.78$ wt%; Young, 2002). This is more commonly associated with the older, "Sturtian" (e.g. Hoffman et al., 2017), part of the Cryogenian Period but is not diagnostic of age (Lechte et al., 2018). Providing a minimum depositional age for the Mineral Fork Formation of the study area, the incision along its upper boundary has been assigned to the regional Upper Caddy Canyon sequence boundary (Levy et al., 1994), which is older than 580 ± 7 Ma (Crittenden and Wallace, 1973; recalculated by Bond et al., 1985).

In summary, the Big Cottonwood Formation was deposited during the late Tonian. Enough time then elapsed to allow its burial and consolidation prior to incision. It is not known whether Mineral Fork Formation deposition occurred immediately after or millions of years after this incision. Relying upon regional correlations, deposition of the Mineral Fork Formation is bracketed between the late Tonian and 580 ± 7 Ma. Most authors, however, presume a Cryogenian age.

1.1.3. Previous work and terminology used in this paper

According to Blick (1979), the purported pavement in Mill B North Fork comprises two parts: (1) two erosional ridges of metre-scale length and height and (2) an adjoining grooved surface with millimetre-depth, metre-length grooves (Fig. 3 A). It was reasoned that, because the grooves cut across bedding, they are the result of subglacial erosion. These "subglacial grooves" were interpreted as Cryogenian, rather than Pleistocene, as their trend is normal to the presumed direction of Pleistocene ice flow. The grooves could not be traced beneath strata of the Mineral Fork Formation. This "subglacially grooved" surface could equally be referred to as a "subglacially striated" surface. As the erosional ridges run parallel to the "subglacial grooves", they were interpreted as Cryogenian "roches moutonnées". One erosional ridge was smaller than the other, forming subordinate relief upon the larger ridge's flank (Fig. 3 A). Most of the data of Blick (1979) are reproduced in Christie-Blick (1983) and Christie-Blick (1997).

For clarity we have slightly modified the terminology used by Blick (1979) (Fig. 3). We treat the two "roches moutonnées" of Blick (1979) together as one feature, named the "roche moutonnée" ridge (Figs. 2 B; 3). We refer to the "roche moutonnée" ridge and adjoining grooved surface collectively as the "pavement" (Figs. 2 B; 3). The following terms are used to divide the "pavement" into specific sections: the "roche moutonnée" ridge; northern side of the "roche moutonnée" ridge; southern side of the "roche moutonnée" ridge; "roche moutonnée" ridge axis; grooved surface. These terms are defined in Figs. 2 and 3 and used throughout the remaining text.

2. Methods

Fieldwork was undertaken in the Big Cottonwood Canyon area during October 2019. In addition to traditional field based measurements and observations, multiple overlapping images were taken for Uncrewed Aerial Vehicle (UAV) photogrammetry using a DJI Mavic Pro UAV and for terrestrial photogrammetry using a Fuji X-T3 digital camera. UAV images relied upon UAV GPS whereas terrestrial photogrammetry used printed ground control points. Photogrammetric point clouds and resulting textured mesh models, digital elevation models and orthomosaic images were built using Agisoft Metashape (2020). Geometric measurements were extracted from point-clouds using Cloudcompare (2020), including use of the qCompass (Thiele et al., 2017) and qFacets (Dewez et al., 2016) plugins. Point cloud-based surface orientation measurements have only been reported where surface (s) within the same model have been ground-truthed using a compass clinometer. Orientations are reported in the format (dip direction°/dip angle°). Intersection lineations were checked using the Stereonet 10 software (Allmendinger et al., 2011; Cardozo and Allmendinger, 2013).

3. Observations and interpretations

3.1. Observations

The "pavement" is a subaerially exposed rock surface that has been exhumed within the last ten million years. It has experienced the same, geologically recent, erosional and neotectonic process as other rock surfaces in the surrounding landscape and at least some of its geomorphological features will undoubtedly record these processes. Our task is to determine whether any of its geomorphological features also record subglacial erosion during an earlier, Precambrian, exposure. To do so we describe: (1) features previously attributed to Cryogenian subglacial erosion i.e. the "roche moutonnée" ridge and "subglacial grooves" (3.1.1); (2) non-glacial sedimentary (3.1.2) and tectonic (3.1.3) structures of the "pavement" that contribute to its geomorphology; (3) features from the surrounding modern landscape resembling those features of the "pavement" that have been attributed to Cryogenian subglacial erosion (3.1.4).

Within the Supplementary Data, animated models of the "pavement" and Mill B North Fork are provided to aid visualisation, along with a high resolution digital elevation model and orthomosaic. Additionally, although beyond the aim of this study, the Supplementary Data provides new outcrop observations and interpretations from the area of the purported Precambrian pavement in Mill B South Fork. These data are consistent with the tectonic re-interpretation of that purported Precambrian pavement, as proposed by Christie-Blick (1982).

3.1.1. "Roche moutonnée" and "subglacial grooves"

In Mill B North Fork, the lithological contrast between the resistant, non-friable, Big Cottonwood Formation and the overlying, friable, Mineral Fork Formation forms a break in slope; from hillside above the break to a cliff face below it (profiles A-B and C-D of Fig. 1 D). The Big Cottonwood – Mineral Fork formation boundary approximately coincides with this break but locally diverges by at least several metres. Along parts of the break, exposed surfaces of the Big Cottonwood Formation protrude from the hillside to form a resistant lip. The "pavement" occurs upon the topographically highest point of one of these lips (profile A-B of Fig. 1 D). The lip in question is a steeply NE-dipping bedding surface (056°/56°) that protrudes westward from the hillside by up to 10 m and continues north–south for 45 m (Fig. 2 A-C). The hillside directly overlying this surface is recessive and exposes no strata (Fig. 2 A-D). At the lowest (northern) end of the surface, this area of non-exposure is overlain by further strata of the Big Cottonwood Formation (Fig. 2 C). Above the "pavement", at the highest (southern) end of the surface, the area of non-exposure is overlain by isolated exposures of the

Table 2
Orientations of key linear features reported in this study.

Feature	Azimuth	Plunge	Figure
"Roche Moutonnée" ridge axis	130°	13°	2, 3, 4
"Subglacial Grooves"	130°/310°	–	4, 5
Cross-set boundaries on grooved surface	130°/310°	–	4, 6
Slickensides on grooved surface	114°/294°	–	6
Fault grooves passing beneath BCF	147°/327°	–	5
Ridge-in-groove on BCF	113°/293°	–	5
Ridges on surface B	125°	5° to 16°	9
Ridges on 100 m scale staircase	122°	25° to 35°	10

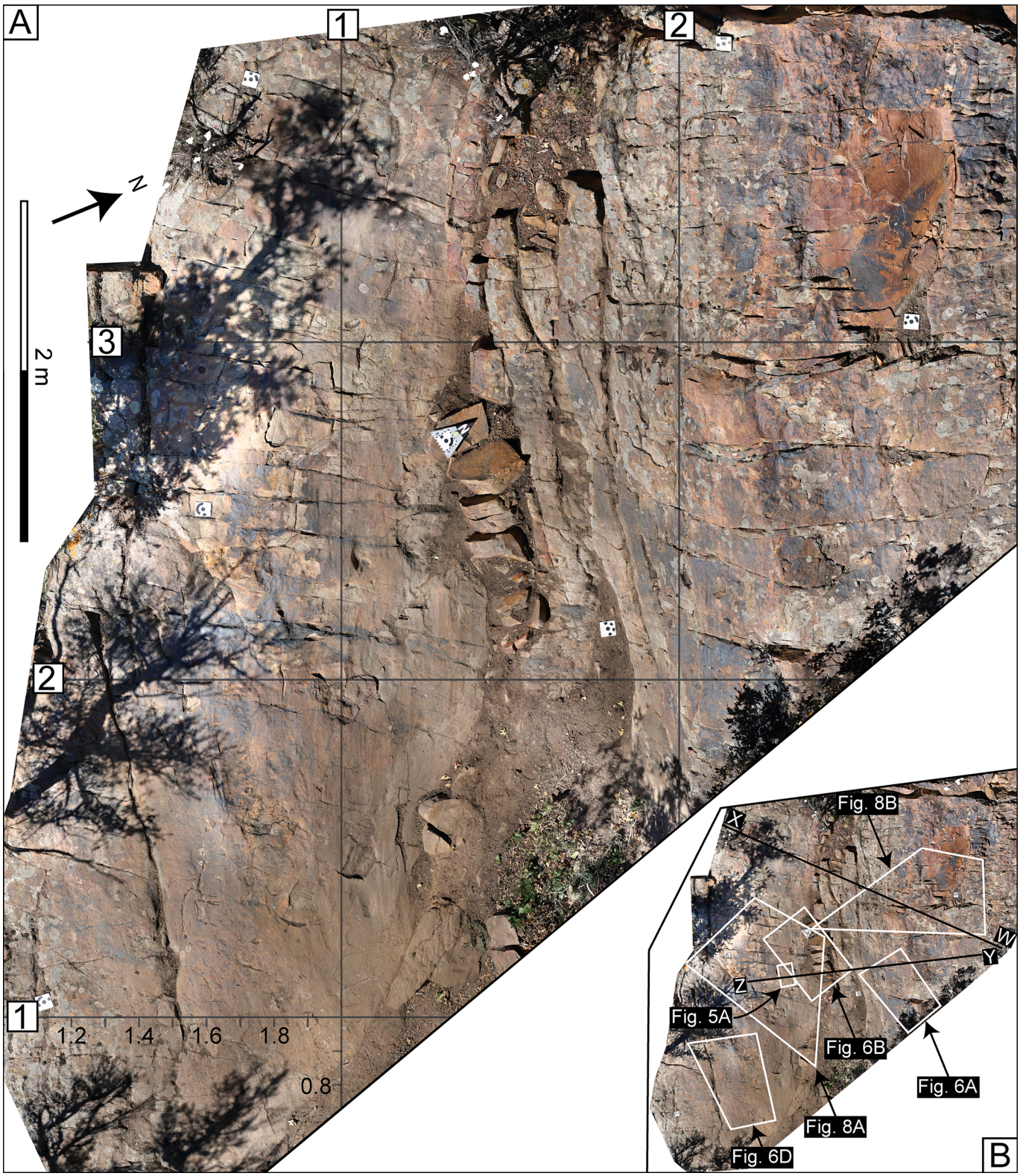

Fig. 4. Orthomosaic of the Mill B North Fork "pavement", comprising the grooved surface, southern side of the "roche moutonnée" ridge and part of its northern side. A: Orthomosaic with arbitrary grid. Grid positions are referred to in the text in [X, Y] format. B: Reduced size figure indicating positions of Figs. 5A; 6A, B, D; 8A, B and profiles W-X and Y-Z from Fig. 3. A high resolution version of this image is available in Fig. S7 of Supplementary Data. The position of this figure is indicated in Fig. 2 C. Orthomosaic built from 1039 terrestrial images, using the same point cloud as Fig. 3D. Nominal image resolution of 0.24 mm/pix.

Mineral Fork Formation, several metres above (Fig. 2 D). No contact between the Mineral Fork Formation and the "pavement" could be found.

The "roche moutonnée" ridge is formed where the topographically highest (southern) end of the NE-dipping bedding surface has been rounded off by erosion (Figs. 2 A, B; 3). The axis of the "roche

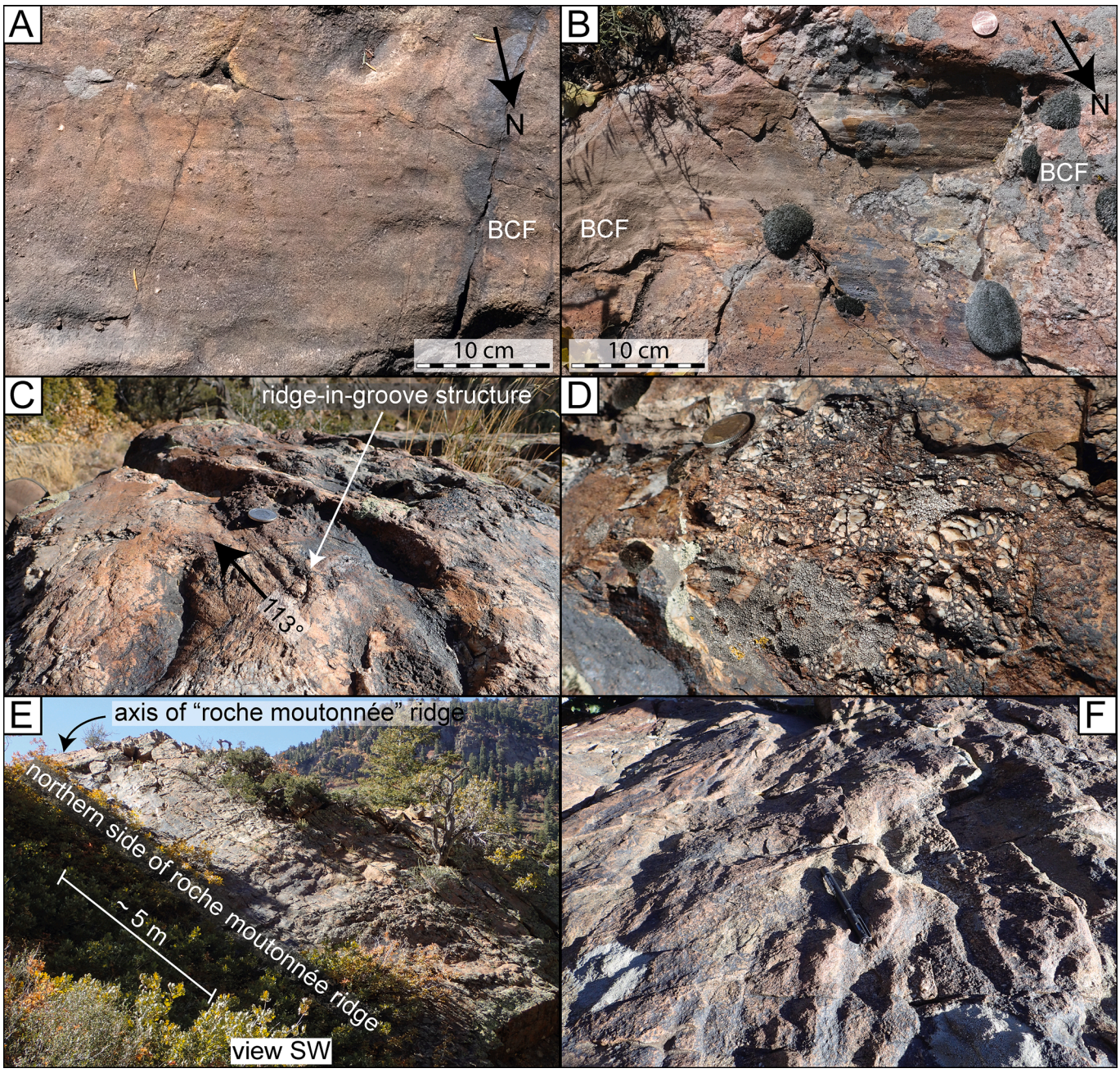

Fig. 5. Erosional and tectonic features of the "pavement" and surrounding landscape. A: The "subglacial grooves". These are the exact same "subglacial grooves" shown in Fig. 59C of Blick (1979), Fig. 30 of Christie-Blick (1983) and Fig. 17a of Christie-Blick (1997). Position given in Fig. 2 E, F; Fig. 4 and Fig. 8 D. B: Fault grooves passing beneath the Big Cottonwood Formation. These occur on the same break in slope as the pavement. Subfigures A and B are shown at identical scales for comparative purposes. Position given in Fig. 1 D. C: Tectonic ridge-in-groove structure within metres of B. Location shown in Fig. 1 D.D: Cataclastic material closely associated with C. Location shown in Fig. 1 D.E: The northern side of the "roche moutonnée ridge" as it transitions northwards, downslope, into a bedding parallel surface. Note the partially abraded texture, better developed towards lower half of the image. Position given in Fig. 2 C. F: Partially abraded surface further along the break in slope. Position given in Fig. 1 D.

moutonnée" ridge (Fig. 3 B) is ~5 m long and plunges gently towards the SE (130°/13°) (Table 2). It is truncated by hillside to the SE and by a joint-controlled cliff to the NW (Fig. 2 C-E). The northern side of the "roche moutonnée" ridge is sub-horizontal where it joins the ridge axis (Figs. 2 D-F; 3B-D). Northward, it steepens to form a ~12 m long, gently convex transition into the remaining, bedding-parallel part of the NE-dipping surface (Fig. 5 E). The southern side of the "roche moutonnée" ridge is steep, convex and smooth where not fractured (Fig. 3 B-D). It descends 2.5 m to an abrupt break in slope, which marks the edge of the adjoining grooved surface.

The grooved surface is similarly oriented to the part of the northern side of the "roche moutonnée" ridge that joins the ridge axis, resulting in a step-like geometry (Fig. 3 B). It is truncated by cliffs, a metre beneath which 057°/45° bedding was measured. The grooved surface is partially obscured by a dark brown patina (Fig. 4). This gradually transitions into a yellow-grey fresh surface that exposes well-sorted, typically medium-grained, meta-sandstone of the Big Cottonwood Formation. The surface has an irregular cm-scale topography with an increasingly karst-like or blistered appearance where the patina is strongest (e.g. grid position [0.8, 2.2] of Fig. 4 A). The "subglacial grooves" are visible in an area of

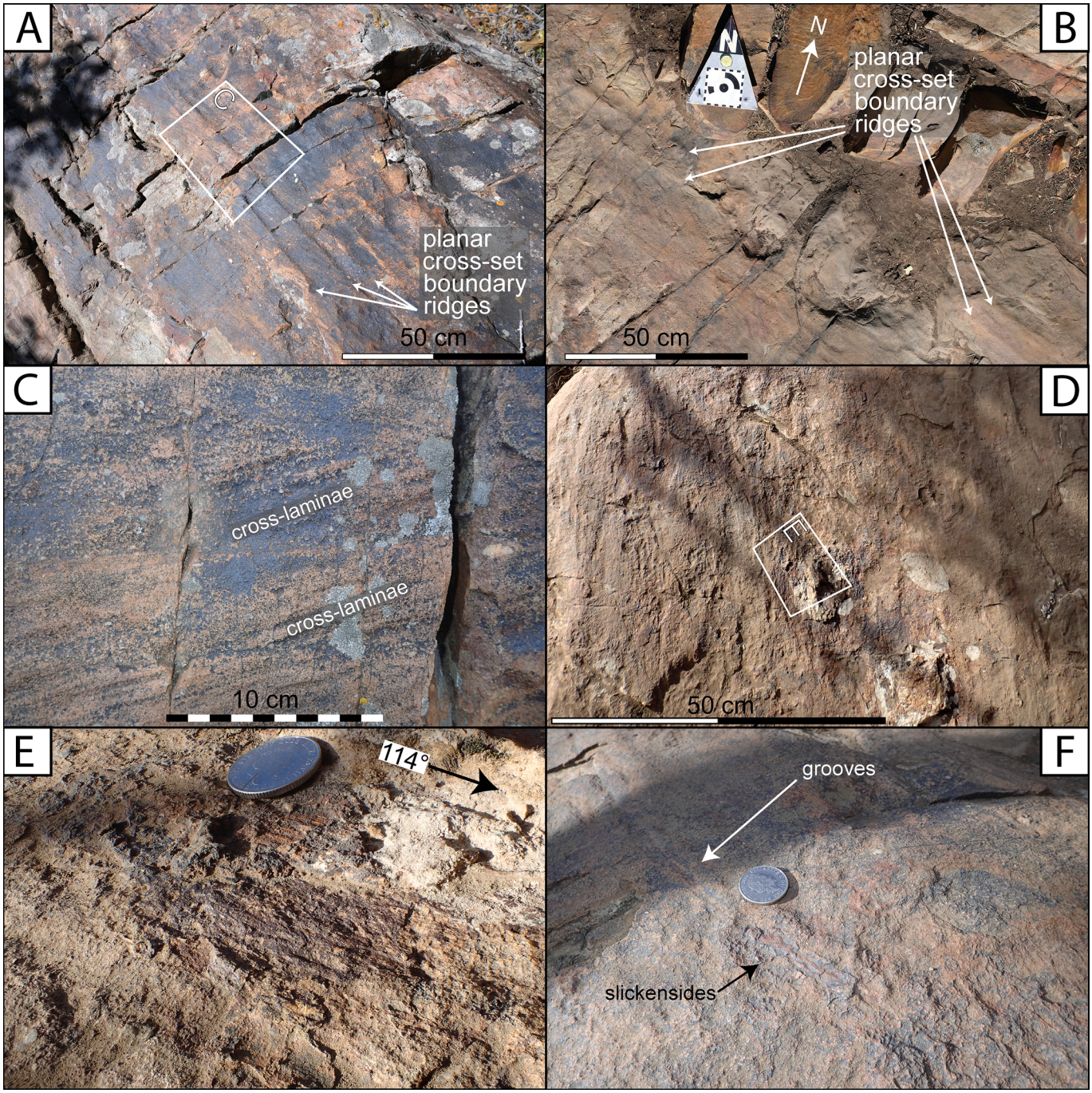

Fig. 6. Sedimentary and tectonic features of the "pavement".A: Small ridges, up to 1 cm high, formed by differential weathering of tabular cross-set boundaries on the southern side of the "roche moutonnée" ridge. Position given in Fig. 4. B: Similar cross-set boundary ridges to A but upon the grooved surface. Position given in Fig. 4. C: Detail of cross laminae from A. Position given in Fig. 6B. D: Mineralised layers hosting slickensides. Patches of plastered material are likely cataclastic material. Position given in Fig. 4. E: Detail of slickensides from D. Position given in Fig. 6D. F: Slickensides merge into grooves.

weak patina (centred at grid position [2.1, 2.3] of Fig. 4 A). The specific examples of "subglacial grooves" shown in Fig. 59C of Blick (1979) are shown in Fig. 5 A (also shown in Figs. 30 and 17a of Christie-Blick, 1983 and Christie-Blick, 1997 respectively). These are straight to very slightly curved, reach ~1 mm depth, ~5 mm width, several dm length and trend ~130°/ 310°, which is parallel to the "roche moutonnée" ridge axis (Table 2).

3.1.2. Sedimentary structures of the "pavement" and the overlying Mineral Fork Formation

Upon the southern side of the "roche moutonnée" ridge, straight to slightly concave, low angle cross-laminae of the Big Cottonwood Formation form planar-based, tabular to wedge-shaped sets of typically 6 to 10 cm thickness (terminology of Mckee and Weir, 1953) (Fig. 6 A, C). The apparent dip of these cross-laminae is mostly NW but occasionally NE or horizontal. Differential weathering has preserved cross-laminae as ridges up to ~1 mm high (Fig. 6 C). By contrast, cross-set boundaries form more pronounced ridges, up to ~1 cm high (Fig. 6 A). These cross-set boundary ridges also occur on the grooved surface, where they trend parallel to the subglacial grooves (~130°/310°), which is the expected intersection lineation between 057°/45° bedding and the grooved surface (e.g. grid position [2.2, 2.8] of Figs. 4; 6 B; Table 2; Supplementary

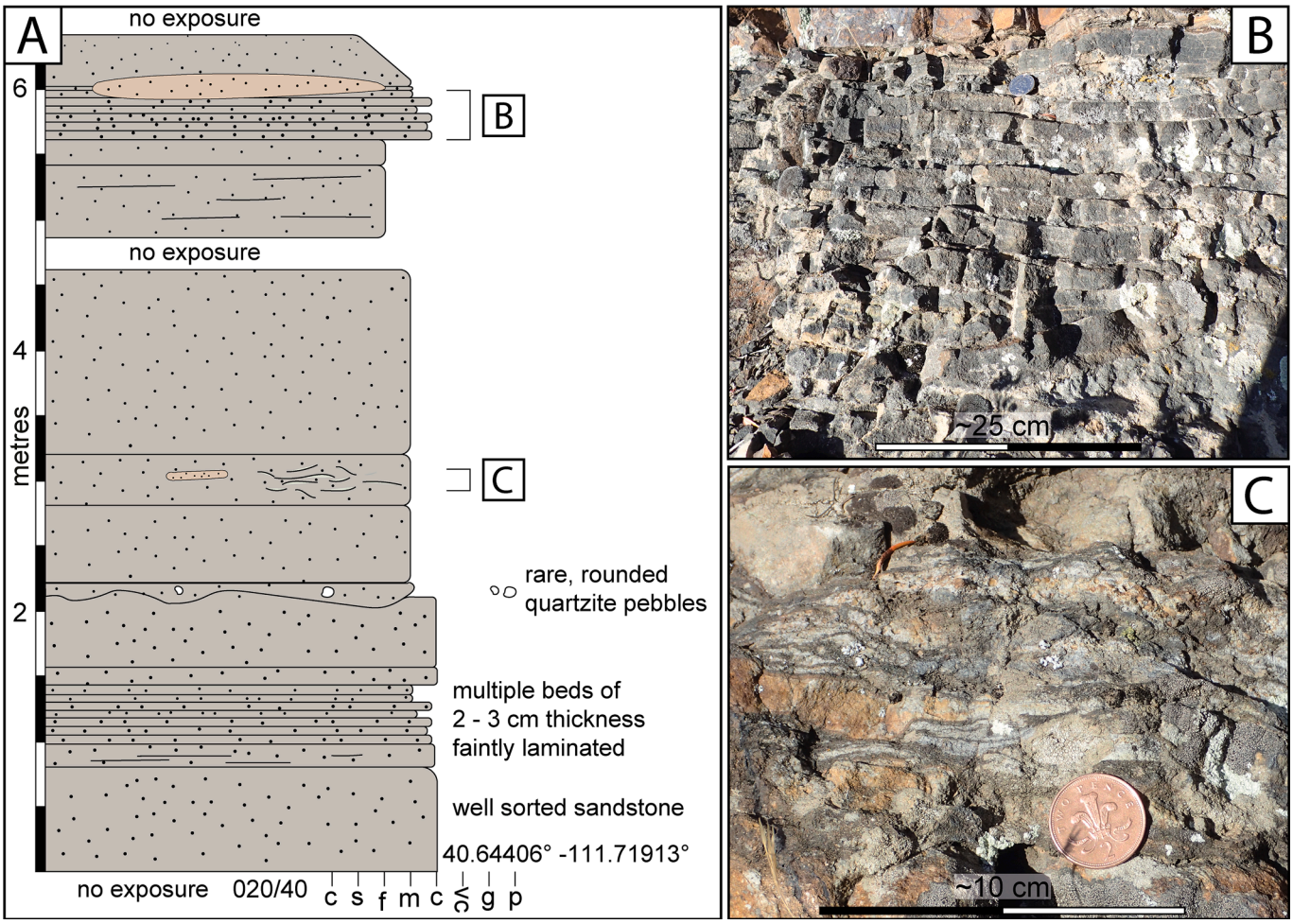

Fig. 7. Example of a better exposure of the Mineral Fork Formation in Mill B North Fork, ~75 m upslope from the break in slope. Position given in Fig. 1 D. A: Measured section. Abbreviations. c: clay, s: silt, f/m/c/vc: fine/medium/coarse/very corase sand, g: granules, p: pebbles. B: Centimetre-scale sandstone beds without lonestones. Coin for scale, diameter 2.45 cm. C: Wisps of sand within a dm-scale bed containing sand lenses. Coin for scale, diameter 2.59 cm. Positions of B and C are given in A.

Data). Unambiguous identification of cross-laminae upon the grooved surface is problematic on account of the surface's irregular topography and patina.

Above the "pavement", but not observed in contact with the "pavement", the stratigraphically lowest Mineral Fork Formation exposure comprises friable, intermittently exposed, poorly-sorted greywacke with occasional pebbles. Around 75 m upslope from the "pavement", the exposure improves and displays a different character of sedimentation. This comprises a proud-weathering section of well-bedded, sorted, fine to coarse grained, massive to laminated sandstone (Figs. 1 D, 7).

3.1.3. *Tectonic features of the "pavement"*

A slickenside surface partially covers the SE part of the grooved surface (grid position [0, 1] of Fig. 4; Fig. 6 D, F). It comprises a dark, <1 mm thick, mineral layer with lineation trending 114°/294° and sub-mm steps descending ESE (Fig. 6 D, E; Table 2). Towards the WNW the slickensides transition into grooves that are up to ~1 cm wide and ~1 mm deep (Fig. 6 F).

A steeply-dipping orthogonal joint system occurs across the "pavement", comprising a well developed NE – SW striking master set and a younger, less well developed, NW – SE cross-joint set (e.g. grid position [1.8, 2.5] of Fig. 4). These are approximately parallel to the cliffs that truncate the "pavement". Less regular fractures with a shallower dip and a larger, cm-scale, aperture pass into the southern side of the "roche moutonnée" ridge and grooved surface (e.g. grid positions [2.8, 2.8] and [1.4, 2.0] of Fig. 4).

Across the "pavement", the rims of fractures vary from sharp to rounded, which is typical of a "partially abraded surface" (typology of Richardson and Carling, 2005). An important demonstration of this can be seen in two distinctively similar depressions (Fig. 8). One adjoins the northern side of the "roche moutonnée" ridge axis and the other occurs upon the grooved surface. The former is up to ~20 cm deep and has a sharp rim to the north but a smoother rim to the south (Fig. 8 A, C). The latter has a smoother rim throughout (Fig. 8 B, D). Nevertheless, the rims of both depressions feature the same saw-tooth planform, defined by the orthogonal joint system. The only other notable difference is between the basal surfaces of the two depressions. The depression adjoining the northern side of the "roche moutonnée" ridge axis has plumose structures along its base, with arrest lines convex towards the SSW to SW (Figs. 4; 8 A, C). The depression upon the grooved surface hosts the "subglacial grooves" but no plumose structures (Figs. 5 A; 8 B, D)

3.1.4. *Features of the surrounding landscape*

The surrounding landscape provides analogous features to the "pavement" at three scales of observation, the mm to cm-scale, the metre to 10 m scale and the 100 m scale.

At the mm to cm-scale, there are grooves with a similar trend (147°/327°) and appearance to the "subglacial grooves" (compare Fig. 5 A and B). Like the "subglacial grooves", these are situated upon an exposed surface of the Big Cottonwood Formation and within metres of the Big

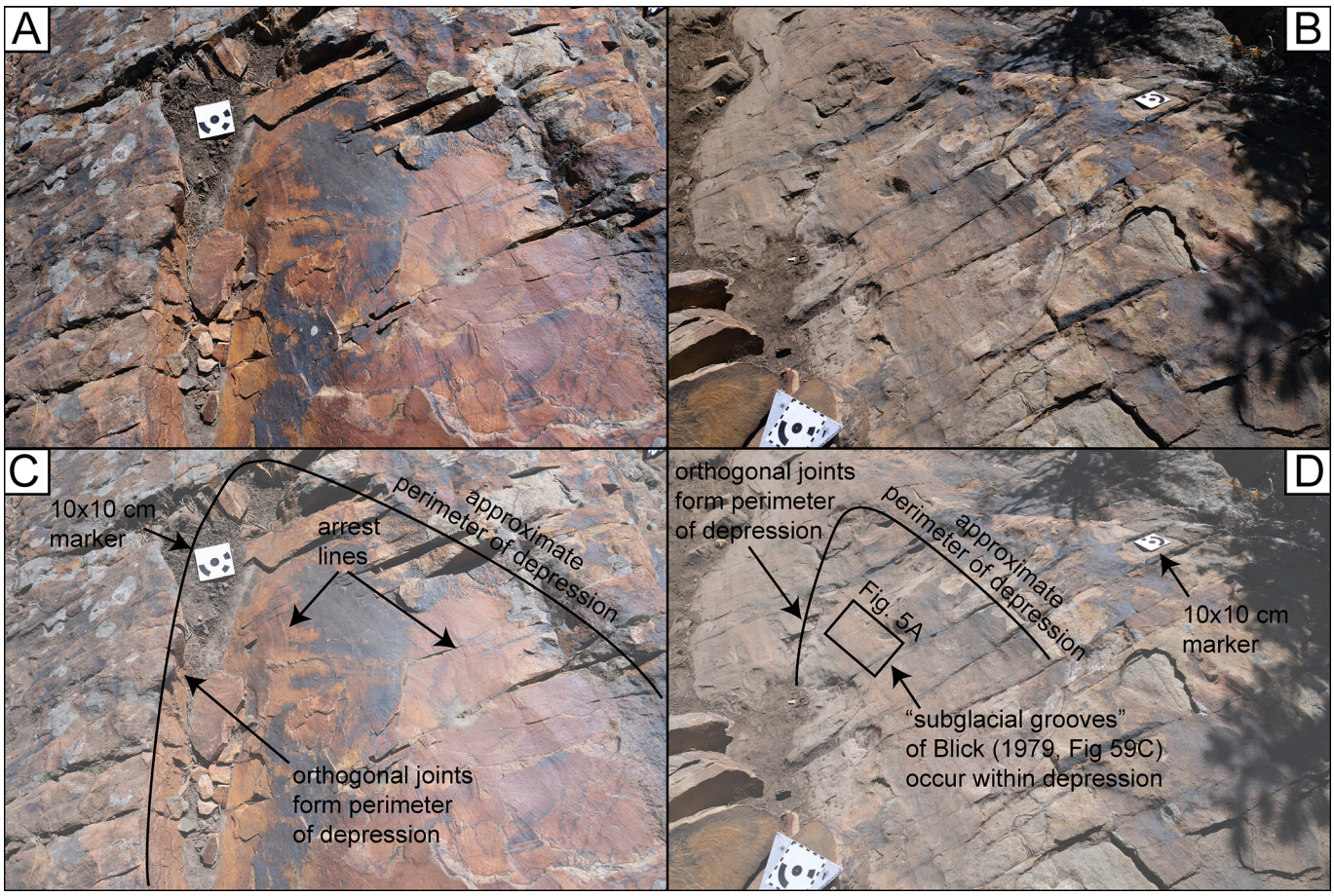

Fig. 8. Comparison between the depression adjoining the northern side of the "roche moutonnée" ridge axis (A, C) and the depression upon the grooved surface (B, D). White square marker is 10 × 10 cm. Position given in Figs. 2F and 4.

Cottonwood – Mineral Fork Formation boundary. However, unlike the "subglacial grooves", these pass beneath further strata of the Big Cottonwood Formation and are therefore undoubtedly fault grooves, not subglacial grooves. Within metres of these grooves is a cm-width tectonic ridge-in-groove structure of a similar trend (113°/293°) to the "subglacial grooves" and associated with cataclastic material (Fig. 5 C, D; Table 2).

Along the remainder of the break in slope, other exposed surfaces of the Big Cottonwood Formation tend to form partially abraded surfaces (typology of Richardson and Carling, 2005) that are comparable to the partially abraded surface of the "pavement" (compare Fig. 5 E and F). Notably, however, some of these other partially abraded surfaces are overlain by further strata of the Big Cottonwood Formation and the partial abrasion cuts across stratigraphic levels. This indicates that the partial abrasion most likely developed since or during the most recent exhumation of the landscape (≤10 to 5 Ma).

At the metre to 10 m scale, the topographically highest (southern) end of another exposed NE-dipping (048°/54°) bedding surface of the Big Cottonwood Formation has been rounded off by erosion, in a similar manner to the "pavement" (40.64325°−111.71935°; Figs. 1 D, 9). We refer to this rounded off part as Surface B. The nearest Mineral Fork Formation exposure is around 10 m from Surface B and it is unclear whether Surface B represents the Big Cottonwood - Mineral Fork Formation boundary or a lower stratigraphic level within the Big Cottonwood Formation. Whereas the surface of the "pavement" is only partially smooth and covered by patina, Surface B is entirely smooth and has a strong patina throughout. Traces of bedding may be distinguished but in general the patina obscures detail. Surface B features smooth, ~ 10 m long ridges and depressions of several metres relief and width. Ridgelines plunge towards 125° at 5° to 16° (Fig. 9 B), which is similar to the 130°/13° plunge of the "roche moutonnée" ridge (Table 2) and parallel to the strike of the adjacent joint-controlled cliffs (Fig. 9 C). A distinct dm-width parallel-sided furrow descends approximately eastward down the lower part of the surface (typology of Richardson and Carling, 2005). This cuts across the ridges and is at least partly formed along a fracture (Fig. 9 A-C). Within Mill B North Fork, we observed no other surfaces that were smoothed and rounded to the same extent as Surface B or the "pavement".

At the 100 m scale, the step-like geometry of the "pavement" (Figs. 2A, B; 3 B, C) also occurs within the surrounding landscape. This is illustrated on the opposite side of the Mill B North Fork valley to the "pavement", where the Big Cottonwood Formation forms a staircase of 100 m scale exposed bedding surfaces separated by cliffs (Fig. 10). The intersections between these bedding surfaces and adjoining cliffs form ridges that are comparable to the "roche mountonée" ridge axis. These ridges plunge towards ~ 122°, which is a similar orientation to both the "roche moutonnée" ridge axis and the ridges of Surface B (Fig. 10, Table 2).

3.2. Interpretation

The presence of grooves upon the "pavement" was taken by Blick (1979) as evidence of subglacial erosion. However, some fault surface processes are analogous to those of subglacial erosion and produce identical products (Fig. 11 A, B). These include fault grooves, crescentic fractures, flute ridges, nail head striation and striated clasts (Eyles and Boyce, 1998; Atkins, 2003). Discriminating between subglacial and tectonic origins for these features therefore relies upon their context

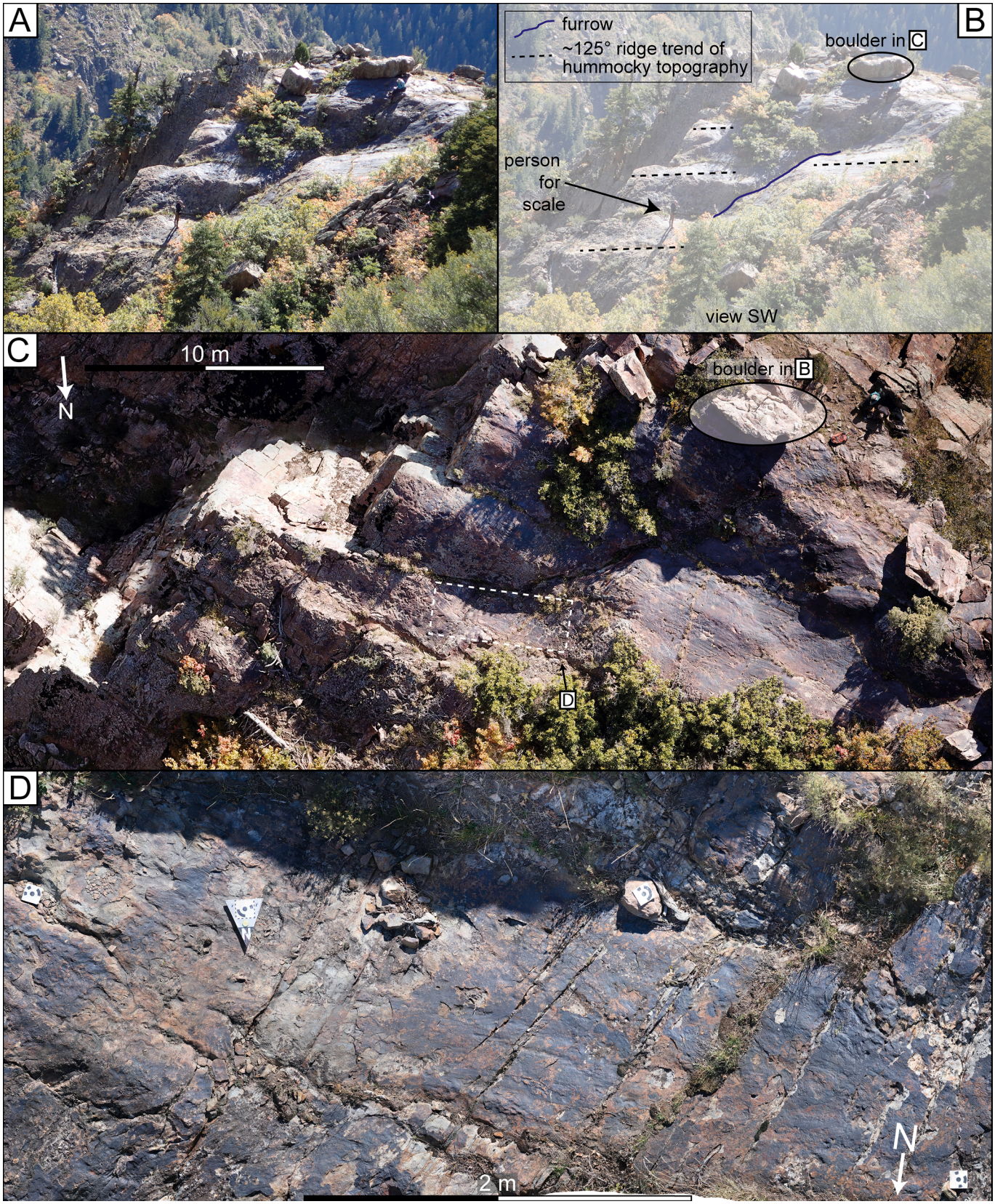

Fig. 9. Surface B. A, B: Oblique view towards the SW, showing furrow and ridges. C: Orthomomosaic built from 366 UAV images with a nominal resolution of 4.36 mm/pixel. Position indicated in Figs. 1 D, 2D. D: Orthomosaic, showing detail of surface, Built from 352 terrestrial image with a nominal resolution of 0.307 mm/pixel. Position indicated in C.

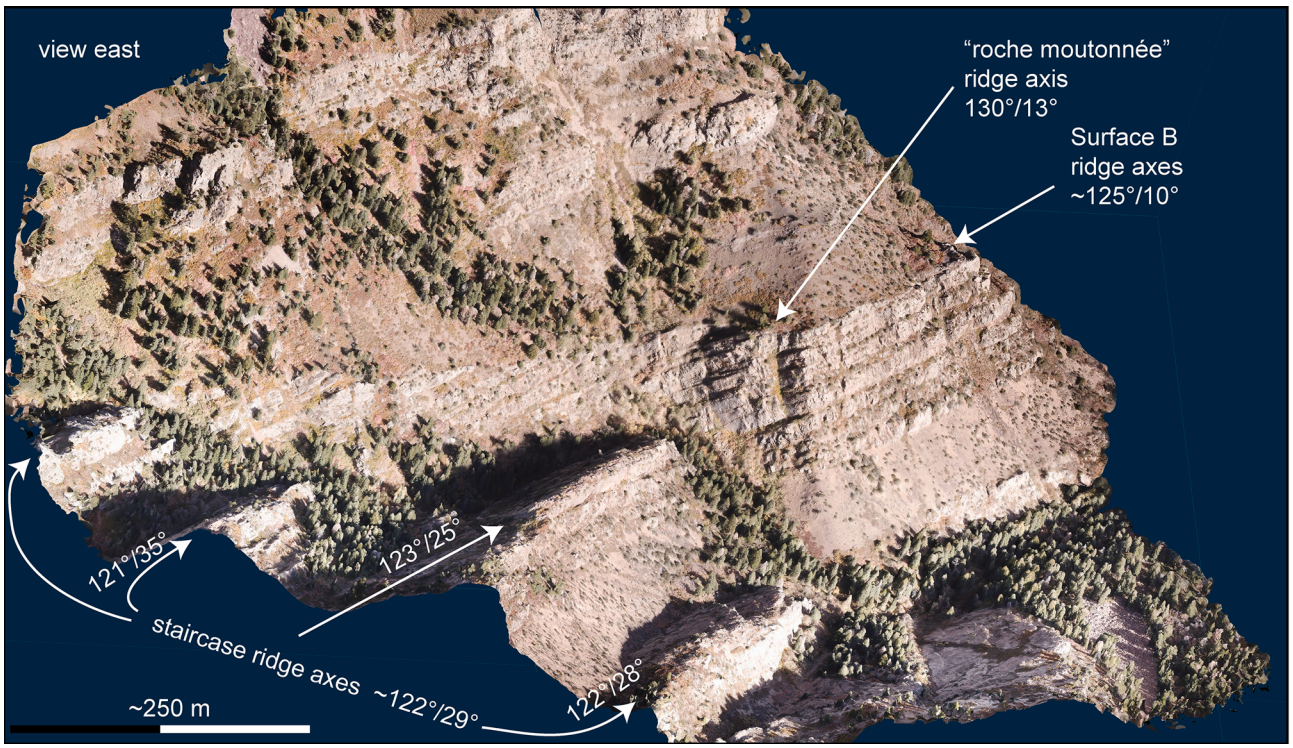

Fig. 10. Mill B North Fork, staircase of 100 m scale exposed bedding surfaces separated by cliffs (lower left of figure). For comparison, the axes orientations of the ridges formed along this staircase and the axes orientations of the "roche moutonnée" and Surface B ridges are labelled. Also compare the step-like geometry of the staircase to the "pavement" (see Figs. 2, 3). Figure created from a UAV point cloud constructed from 1340 images, staircase ridge orientations measured using qCompass (Thiele et al., 2017) in Cloudcompare (2020).

rather than the characteristics of the features themselves (Fig. 11 C, D). The morphology of the "subglacial grooves" is consistent with either a subglacial or tectonic origin. However, contextual evidence from both the "pavement" and surrounding landscape strongly suggests a tectonic origin.

Upon the "pavement", slickensides that transition into grooves confirm that at least part of the grooved surface was a fault surface (Fig. 6 D-F). It is unlikely that these slickensides are instead subglacial striae as their stepped, perfectly parallel form is quite unlike the unequivocal Pleistocene subglacial striae formed upon strata of the same formation in Mill B South Fork (Supplementary Data; Fig. S5). Additionally, neither the mineral layer that hosts the slickensides nor the patina upon the "pavement" resemble glacial polish, which often accompanies subglacial striae. Glacial polish frequently weathers in a characteristic manner, peeling off as mm-thickness circular patches (Siman-Tov et al., 2017). This applies equally to recent and Precambrian subglacially striated surfaces, which may be identical in appearance (e.g. compare Fig. 1A of Siman-Tov et al., 2017; and Fig. 11D of Vandyk et al., 2019). Glacial polish upon Pleistocene striated surfaces of the Big Cottonwood Formation in Mill B South Fork exhibits this classic weathering pattern and provides an indication of the appearance that would be expected of glacial polish upon the "pavement" (Supplementary Data; Fig. S5). This appearance is quite unlike the stepped weathering of the slickenside-hosting mineral layer on the "pavement" or the gradual lateral transitions of its patina.

Only a short distance from the "pavement", the fault grooves (Fig. 5 B) are analogous to the "subglacial grooves" in almost every sense (Fig. 5 A). This includes their position on the break in slope, lithology and overall appearance. The key difference is that the fault grooves pass beneath overlying Big Cottonwood Formation strata, confirming their tectonic interpretation, whereas no overlying strata are preserved in contact with the "pavement". The orientation of the "subglacial grooves" (~130°/310°) is also consistent with a tectonic origin. It is midway between the fault grooves (147°/327°) and both the tectonic ridge-in-groove structure (113°/293°) and the slickensides on the grooved surface (114°/294°) (Figs. 5, 6; Table 2).

In addition to fault-related processes, considerable precipitation running off the hillside has had a significant erosional influence upon the landscape of the study area (Stock et al., 2009; Quirk et al., 2018). In this context, the partially abraded texture found along the break in slope, which occurred during or since the most recent exhumation (≤10 to 5 Ma), records competing erosional processes (Fig. 5 F). On the one hand, fluvial plucking or subaerial weathering exploit the densely jointed nature of the landscape to produce angular features; on the other hand, fluvial abrasion or dissolution processes tend to smooth and round features (Richardson and Carling, 2005; Wray and Sauro, 2017; Scott and Wohl, 2019). As part of the same break in slope, some or all of the partial abrasion on the "pavement" must also have been produced by these same erosional processes, during or since the most recent exhumation (≤10 to 5 Ma).

Upon the basal surface of the depression that adjoins the "roche moutonnée" ridge axis, arrest lines record the incremental propagation of an opening mode fracture plane (Ziegler et al., 2014) (Figs. 4, 8 A, C). The intersection between this sub-horizontal opening mode fracture and the sub-vertical orthogonal joint system, which defines the depression's perimeter, has liberated a slab of the Big Cottonwood Formation. This slab was then removed to create the depression. Given the clear evidence for geologically recent widespread abrasion along the break in slope, the sharp (i.e. unabraded) northern rim of the depression confirms that it is a geologically recent feature. Most likely the removed slab has now simply fallen down-slope, perhaps aided by run-off or seismicity (e.g. Pang et al., 2020). The similarity between this depression and the depression upon the grooved surface strongly suggests a common process and age of formation (compare Fig. 8 A, D with B, D). In this case, the part of the grooved surface within the depression was only exposed in the geologically recent past, not during the Precambrian, and the

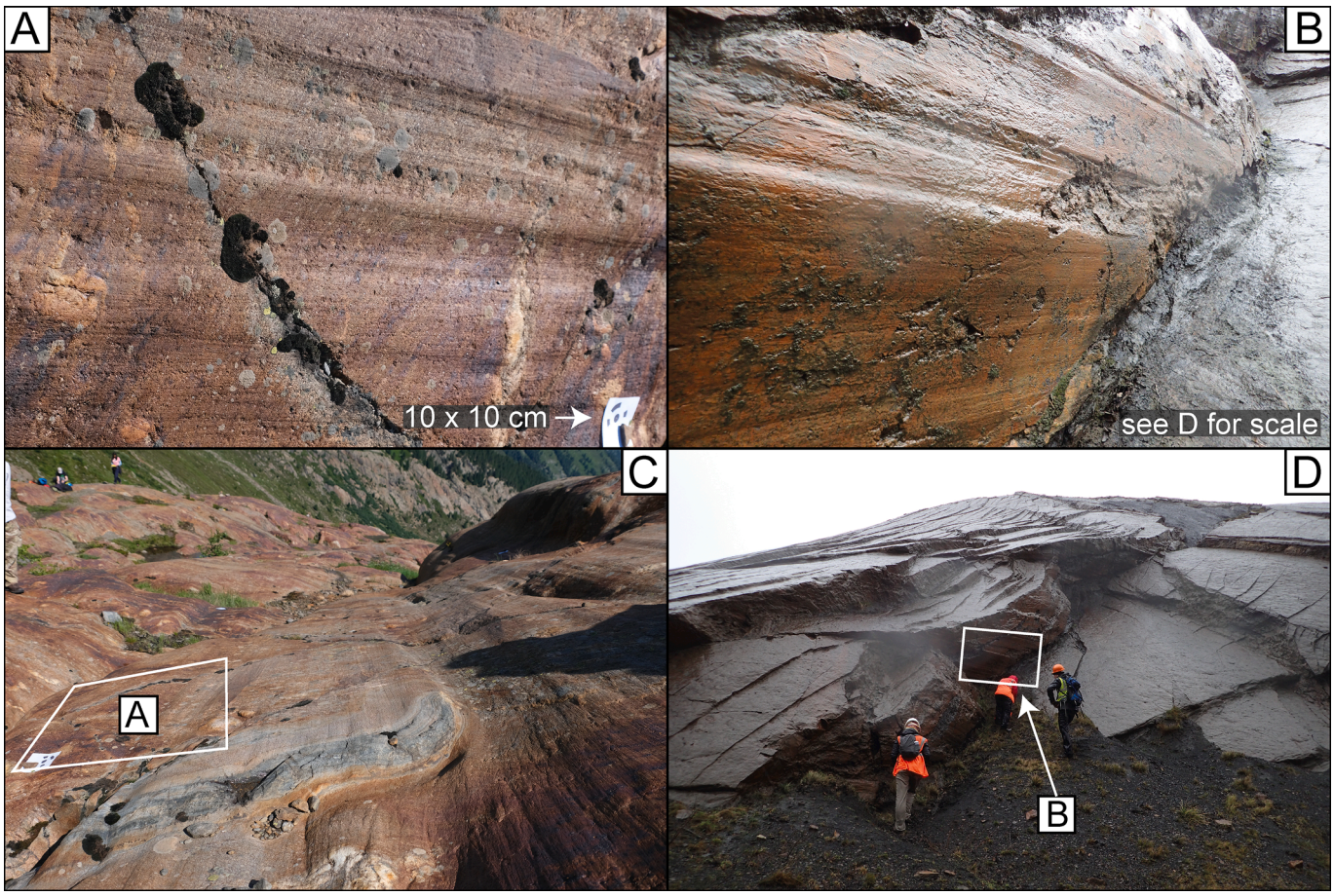

Fig. 11. An example of the similarity between subglacial and fault features. Distinguishing between A (subglacial grooves) and B (fault grooves) is only possible when their contexts are revealed, which are shown in C and D respectively. A: Subglacially striated surface revealed form beneath Gepatsch glacier at Kaunertal, Austria, within the last century. B: Grooved fault surface on Carboniferous strata at Spireslack Quarry, Scotland. Reflection is due to rain. C: Striated surface from A in context, revealing that it is a subglacial feature. D: Grooved fault surface from B in context, revealing it is a tectonic feature. Note people for scale in C and D.

"subglacial grooves" upon it cannot be the product of Precambrian subglacial erosion. This is consistent with the reinterpretation of the "subglacial grooves" as fault grooves produced by sliding of the removed slab.

In comparison to the "pavement", the better developed smoothing, rounding and patina of Surface B demonstrate that abrasion has dominated. The furrow and smooth, rounded ridges of Surface B are typical of either fluvial abrasion in an open bedrock channel (e.g. Richardson and Carling, 2005) or subglacial erosion of an S-form (e.g. Shaw et al., 2020). The fluvial explanation is more likely. First, there is a lack of subglacial striation or glacial polish, which are most often at least partially present upon an S-form. Second, the strong patina, especially well developed on Surface B, has the classic "burnished copper" appearance associated with fluvially polished bedrock surfaces (Richardson and Carling, 2005) and, as described above for the patina on the "pavement", is distinctly different to the glacial polish preserved on strata of the same formation in Mill B South Fork. Third, an S-form of Pleistocene age is particularly unlikely as the angular cliffs, 100 m scale "staircase" geomorphology and v-shaped valley of Mill B North Fork are inconsistent with recent subglacial erosion (compare to Mill B South Fork: Supplementary Data, Fig. S3).

If formed by Precambrian subglacial erosion the "pavement" must represent the Big Cottonwood – Mineral Fork Formation boundary. However, as we could not find any contact between the "pavement" or Surface B and the Mineral Fork Formation, it remains possible that either surface is instead below that boundary. Recessive non-exposure above the "pavement" cannot be assumed to represent the Mineral Fork Formation. This is demonstrated above the northern end of the NE-dipping bedding surface that hosts the "pavement" (Fig. 2 A, B). There, recessive non-exposure, similar to that above the "pavement", is overlain by further strata of the Big Cottonwood Formation.

The fact that the distinctly smoothed texture of Surface B, and to a lesser extent the "pavement", were uniquely observed in proximity to the break in slope, associated with the Big Cottonwood – Mineral Fork Formation boundary, suggests two possibilities. Either the "pavement" and Surface B record Precambrian erosion (not necessarily glacial) upon the Big Cottonwood – Mineral Fork Formation boundary or they record fluvial erosion across the break in slope during or since the most recent exhumation ($\leq$10 to 5 Ma). The geologically recent fluvial explanation is favoured for three reasons.

First, episodic fluvial erosion by run-off is likely to have been enhanced upon the pronounced break in slope where the "pavement" and Surface B protrude (Section A-B and C-D of Fig. 1 D). This is referred to as a knickpoint lip in the fluvial literature (Miller, 1991; Hancock et al., 1998; Richardson and Carling, 2005). In this context the furrow on Surface B is a "chute furrow", typical of such a bedrock step (Richardson and Carling, 2005, p. 38).

Second, the "roche moutonnée" and Surface B ridges are similarly oriented to both the surrounding joint controlled cliffs and the ridges of the 100 m scale staircase. This implies that, although these are all erosional features formed at the Earth's surface, their formation was controlled by the same structural influences, especially the well-

developed cross-joint system (Scott and Wohl, 2019). It is unlikely that the same structural influences existed during any Precambrian exposure, which would have occurred in a different tectonic regime and before tilting of the beds. Therefore these features most likely formed at the Earth's surface during or since the most recent exhumation (≤10 to 5 Ma).

Third, the step-like geometry of the "pavement" is also shown by the 100 m scale staircase. The bench and cliff configuration of the staircase was produced within the geologically recent landscape, as a response to fluvial incision along Mill B North Fork. Similar responses to fluvial incision, within similar meta-sandstone landscapes, are documented in the literature. For example, the Sioux Quartzite (USA) is a Proterozoic, bedded to cross-bedded, meta-sandstone. Where it has been incised by streams, as a result of prominent bedding and joints, it has formed alternating benches and vertical faces that are analogous to the staircase of Mill B North Fork (Southwick et al., 1986; Young et al., 2009). Therefore, processes capable of producing the step-like morphology of the "roche moutonnée" ridge have been active within the surrounding recent landscape. Invoking Precambrian subglacial erosion to explain the metre-scale morphology of the "pavement" is therefore neither necessary nor parsimonious.

3.2.1. Summary

It remains unconfirmed whether the "pavement" and Surface B occur upon or beneath the Big Cottonwood – Mineral Fork Formation boundary. Contextual evidence strongly suggests that the "subglacial grooves" of Blick (1979) are more likely a later tectonic feature than the result of Precambrian glaciation. The part of the grooved surface within the depression is likely a geologically recent feature, in which case the "subglacial grooves" within it cannot be attributed to Precambrian subglacial erosion. The smoothed and rounded parts of the "pavement" and especially Surface B likely record recent bedrock fluvial erosion, resulting from their position upon a break in slope, combined with significant precipitation. The resulting erosional morphologies were formed under the influence of the same structural controls as the surrounding geologically recent landscape (≤10 to 5 Ma). This has resulted in similar orientations between the ridges of the "roche moutonnée", Surface B and the 100 m scale staircase. Since it is unlikely that these same structural controls existed during the Precambrian, this favours a geologically recent explanation for the "pavement" and Surface B. The step-like geometry of the "pavement" may also be explained by geologically recent processes, evident in the 100 m scale staircase and similar meta-sandstone landscapes in the literature.

4. Discussion

Without the supporting evidence of the "pavement" we must re-evaluate the incision between the Mineral Fork and Big Cottonwood formations. The steep angle of incision (≤40°) is consistent with either subglacial (Glasser and Bennett, 2004) or bedrock fluvial erosion (Gibling, 2006). Likewise the depth of incision (≤800 m) is consistent with a glacial trough or fluvial incision driven by rift flank uplift (e.g. eastern flank of Kenyan rift: Xue et al., 2019).

As previously described, the incision is insufficiently exposed to determine any diagnostic glacial geometry (Fig. 1 C; Fig. S2 and text of Supplementary Data). Nevertheless, Christie-Blick (1983) proposed a more complex geometric argument to imply subglacial erosion. This relied upon comparison of incision depths between the Mill B North Fork footwall and hanging wall blocks (Christie-Blick, 1983, p. 752, point 3). However, this is problematic as variable incision along the Mineral Fork Formation's upper boundary, exacerbated by faulting and poor exposure of the footwall block, mean that the original incision depth is unknown (Crittenden, 1965a; Crittenden, 1976; Ojakangas and Matsch, 1980; Levy et al., 1994) (Fig. 1 C).

Greywacke, in Mill B North Fork, and diamictite or laminated fine-grained sandstone, in Mill B South Fork, rest upon the incision and may be glacially influenced deposits (Blick, 1979; Ojakangas and Matsch, 1980; Christie-Blick, 1983). However, the presence of glacially influenced strata above an incision does not necessarily indicate subglacial erosion. For example, Quaternary glaciomarine deposits of the Warren House Formation of the UK directly fill fluvial valleys that were incised during non-glacial conditions (Davies, 2008).

In summary, it is just as likely that incision into the Big Cottonwood Formation was caused by fluvial rather than subglacial erosion, potentially under non-glacial climatic conditions. Before the present study, the Big Cottonwood study area was the only point in the Utah – Idaho region where the presence of grounded Cryogenian ice could be asserted with any confidence. From modern glacial grounding lines, debris has been rafted for hundreds or thousands of kilometres by ice shelves or bergs respectively (Andrews, 2000; Talley et al., 2011) and glacially influenced gravity flows have run-out hundreds of kilometres (King et al., 1998; Wilken and Mienert, 2006). Therefore, combining our reinterpretation of the "pavement" with the uncertainties associated with previous tillite interpretations, it is now questionable whether grounded Cryogenian ice was ever present or even near to the Utah – Idaho region.

The possibility of fluvial incision may also help clarify long standing correlation and age uncertainties plaguing the Mineral Fork Formation (Crittenden et al., 1983). Incision above the Mineral Fork Formation in the study area has previously been assigned to the Upper Caddy Canyon sequence boundary (Levy et al., 1994). In their regional lithostratigraphic analysis, Levy and Christie-Blick (1991, their Figure 2) tentatively placed the next sequence boundary below this, namely the Upper Maple Canyon sequence boundary at Huntsville (Fig. 1 B), at a stratigraphic level overlapping the Mineral Fork Formation of the study area (also see Levy et al., 1994). Only minimal modification of their analysis is therefore required to assign the Upper Maple Canyon sequence boundary to the incised Big Cottonwood – Mineral Fork Formation boundary in the study area. If correct, the Mineral Fork Formation of the study area is significantly younger than the glacigenic Perry Canyon Formation, which has a maximum depositional age of 667 ± 5 Ma (Crittenden et al., 1983; Balgord et al., 2013; Yonkee et al., 2014).

In a rift setting, such as the Utah – Idaho region of the Cryogenian, diamictites are frequently deposited by sediment gravity flows, triggered by tectonism. These mass flows alone do not indicate glaciation and have no climatic significance (e.g. Crowell, 1957; Carto and Eyles, 2012). Distinguishing poorly sorted deposits of non-glacial, mass flow origin from those that are ultimately from a glacial source represents a long running challenge to understandings of the extent, duration and severity of Cryogenian glaciation (Kennedy and Eyles, 2020). Prior to our re-interpretation of the "pavement", it was irrefutable that the stratigraphically lowest confirmed evidence for glaciation in the study area was the incised Big Cottonwood - Mineral Fork Formation boundary. Above this, the lowest documented striated clasts and dropstones, which have been considered diagnostic of a glacial influence, are stratigraphically > 300 m higher (Fig. 23 and Table 21 of Blick, 1979). In light of our re-interpretation and the possibility of non-glacial incision into the Big Cottonwood Formation, we must now question whether the lower reaches of the Mineral Fork Formation record glacially influenced deposition or non-glacial, rift-related sedimentation that transitions upwards into glacial conditions. In a global context, this latter possibility serves to reiterate concerns raised by previous authors, that the extent and duration of Cryogenian glaciation may be over-estimated if tectonic and climatic influences are conflated (e.g. Eyles and Januszczak, 2004; Kennedy and Eyles, 2020).

5. Conclusions

The only uncontested Cryogenian "pavement" from the western margin of the Laurentian palaeocontinent and the entire modern North American continent is best explained as a structurally controlled erosional feature of the modern landscape, with no connection to

Precambrian glaciation;

The incision beneath the Mineral Fork Formation, previously presumed to record subglacial erosion, can as easily be explained by fluvial erosion, potentially under non-glacial conditions;

The presence of grounded ice in the Utah – Idaho region during the Cryogenian Period is now unconfirmed;

Building upon the long established consensus that the Mineral Fork Formation strata contain within them multiple sediment gravity flows deposited in a rift setting, it is possible that lower strata of the formation record non-glacial conditions that transition upwards into glaciation.

CRediT authorship contribution statement

T.M. Vandyk: Conceptualization, Methodology, Formal analysis, Writing - original draft, Visualization, Funding acquisition. **C. Kettler:** Methodology, Formal analysis, Visualization. **B.J. Davies:** Supervision, Writing - review & editing. **G.A. Shields:** Supervision, Writing - review & editing. **I. Candy:** Supervision, Writing - review & editing. **D.P. Le Heron:** Supervision, Writing - review & editing, Funding acquisition.

Data Availability

All data are available either in this manuscript or its supplementary materials: https://doi.org/10.17632/ysjtv99rwk.1. https://doi.org/10.17632/ysjtv99rwk.1 is the DOI of the Mendeley data set.

Declaration of Competing Interest

The authors declare that they have no known competing financial interests or personal relationships that could have appeared to influence the work reported in this paper.

Acknowledgments

TMV gratefully acknowledges funding from the Postgraduate Research Grant of the International Association of Sedimentologists, the Postgraduate Research Grant of the British Society for Geomorphology and the Student Research Grant of the Society for Sedimentary Geology (SEPM). This work was supported by the Natural Environment Research Council [grant number NE/L002485/1]. We are most grateful for the constructive review of this manuscript and its previous iteration by 3 anonymous reviewers, Marie Busfield, Nicholas Eyles and Maarten Krabbendam.

Appendix A. Supplementary data

All Supplementary Data can be found at https://doi.org/10.17632/ysjtv99rwk.1.

References

Abbot, D.S., Voigt, A., Koll, D., 2011. The Jormungand global climate state and implications for Neoproterozoic glaciations. J. Geophys. Res.: Atmos. 116 (D18) https://doi.org/10.1029/2011JD015927.

Allmendinger, R.W., Cardozo, N., Fisher, D.M., 2011. Structural geology algorithms: Vectors and tensors. Cambridge University Press.

Andrews, J., 2000. Icebergs and iceberg rafted detritus (IRD) in the North Atlantic: facts and assumptions. Oceanography 13 (3), 100–108. https://doi.org/10.5670/oceanog10.5670/oceanog.200010.5670/oceanog.2000.19.

Armstrong, P.A., Ehlers, T.A., Chapman, D.S., Farley, K.A., Kamp, P.J.J., 2003. Exhumation of the central Wasatch Mountains, Utah: 1. Patterns and timing of exhumation deduced from low-temperature thermochronology data. Journal of Geophysical Research: Solid. Earth 108 (B3). https://doi.org/10.1029/2001JB001708.

Armstrong, R.L., Taubeneck, W.H., Hales, P.O., 1977. Rb-Sr and K-Ar geochronometry of Mesozoic granitic rocks and their Sr isotopic composition, Oregon, Washington, and Idaho. GSA Bulletin 88, 397–411. https://doi.org/10.1130/0016-7606(1977)88<397:RAKGOM>2.0.CO;2.

Cloudcompare - 2.11.0 (Annoia) Stereo, http://cloudcompare.org/ 2020.

Arnaud, E., Etienne, J.L., 2011. Chapter 3 Recognition of glacial influence in Neoproterozoic sedimentary successions. Geological Society, London, Memoirs 36, 39–50. 10.1144/M36.3.

Asklund, B., 1960. Guide to the excursions nos. A24 and C19, in: International Geological Congress, XXI Session Norden, Guide to the Excursions: Studies of the Thrust Region of the Southern Part of the Swedish Mountain Chain. pp. A24, C19.

Assine, M.L., de Santa Ana, H., Veroslavsky, G., Vesely, F.F., 2018. Exhumed subglacial landscape in Uruguay: Erosional landforms, depositional environments, and paleo-ice flow in the context of the late Paleozoic Gondwanan glaciation. Sediment. Geol. 369, 1–12. https://doi.org/10.1016/j.sedgeo.2018.03.011.

Atkins, C.B., 2003. Characteristics of striae and clast shape in glacial and non-glacial environments (PhD Thesis). Victoria University of Wellington.

Atwood, W.W., 1909. Glaciation of the Uinta and Wasatch mountains: Professional Paper 61. US Government Printing Office.

Balgord, E.A., Yonkee, W.A., Link, P.K., Fanning, C.M., 2013. Stratigraphic, geochronologic, and geochemical record of the Cryogenian Perry Canyon Formation, northern Utah: Implications for Rodinia rifting and snowball Earth glaciation. Geol. Soc. Am. Bull. 125 (9-10), 1442–1467. https://doi.org/10.1130/B30860.110.1130/2013257.

Benn, D.I., Evans, D.J.A., 2010. Glaciers and Glaciation, 2nd edition: Taylor & Francis Ltd.

Bennett, M.R., Waller, R.I., Glasser, N.F., Hambrey, M.J., Huddart, D., 1999. Glacigenic clast fabrics: genetic fingerprint or wishful thinking? J. Quat. Sci. 14 (2), 125–135. https://doi.org/10.1002/(ISSN)1099-141710.1002/(SICI)1099-1417(199903)14:2<>1.0.CO;2-410.1002/(SICI)1099-1417(199903)14:2<125::AID-JQS426>3.0.CO;2-0.

Blackwelder, E., 1932. An ancient glacial formation in Utah. J. Geol. 40 (4), 289–304. https://doi.org/10.1086/623953.

Blick, N.H., 1979. Stratigraphic, structural and paleogeographic interpretation of upper Proterozoic glaciogenic rocks in the Sevier Orogenic Belt, northwestern Utah (PhD Thesis). University of California, Santa Barbara.

Bond, G.C., Christie-Blick, N., Kominz, M.A., Devlin, W.J., 1985. An Early Cambrian Rift to Post-Rift Transition in the Cordillera of Western North-America. Nature 315 (6022), 742–746. https://doi.org/10.1038/315742a0.

Bressler, S.L., 1981. Preliminary Paleomagnetic Poles and Correlation of the Proterozoic Uinta Mountain Group, Utah and Colorado. Earth Planet. Sci. Lett. 55 (1), 53–64. https://doi.org/10.1016/0012-821X(81)90086-8.

Cardozo, N., Allmendinger, R.W., 2013. Spherical projections with OSXStereonet. Comput. Geosci. 51, 193–205. https://doi.org/10.1016/j.cageo.2012.07.021.

Carto, S.L., Eyles, N., 2012. Sedimentology of the Neoproterozoic (c. 580 Ma) Squantum "Tillite", Boston Basin, USA: Mass flow deposition in a deep-water arc basin lacking direct glacial influence. Sediment. Geol. 269, 1–14. https://doi.org/10.1016/j.sedgeo.2012.03.011.

Christie-Blick, N., 1997. Neoproterozic Sedimentation and Tectonics in West-Central Utah. In: Link, P.K., Kowallis, B.J. (Eds.), Geological Society of America Field Trip Guidebook Volume 42: 1997 Annual Meeting Salt Lake City, Utah. Proterozoic to Recent Stratigraphy, Tectonics. and Volcanology, Utah, Nevada, Southern Idaho and Central Mexico, pp. 1–30.

Christie-Blick, N., 1983. Glacial-marine and subglacial sedimentation Upper Proterozoic Mineral Fork Formation, Utah. In: Molnia, B.F. (Ed.), Glacial-Marine Sedimentation. Springer, Boston, MA, pp. 703–776.

Christie-Blick, N., 1982. Upper Precambrian (eocambrian) Mineral Fork Tillite of Utah - a Continental Glacial and Glaciomarine Sequence - Discussion. Geol. Soc. Am. Bull. 93, 184–186. https://doi.org/10.1130/0016-7606(1982)93<184:UPEMFT>2.0.CO;2.

Coats, R.P., Preiss, W.V., 1987. Stratigraphy of the Umberatana Group. In: Preiss, W.V. (Ed.), The Adelaide Geosyncline. Late Proterozoic Stratigraphy, Sedimentation, Palaeontology and Tectonics, Bulletin of the Geological Survey of South Australia, pp. 125–209.

Corkeron, M., 2011. Neoproterozoic glacial deposits of the Kimberly Region and northwestern Northern Territory, Australia. Geological Society, London, Memoirs 36, 659–672. https://doi.org/10.1144/M36.65.

Crittenden, M.D., 1976. Stratigraphic and structural setting of the Cottonwood area, Utah. Rocky Mountain Association of Geologists 1976 Symposium.

Crittenden, M.D., 1965a. Geology of the Mount Aire Quadrangle, Salt lake County, Utah. GQ-379.

Crittenden, M.D., 1965b. Geology of the Dromedary peak quadrangle, Utah. GQ-378.

Condie, Kent C., 1967. Petrology of the Late Precambrian Tillite Association in Northern Utah. Geol Soc America Bull 78 (11), 1317. https://doi.org/10.1130/0016-7606(1967)78[1317:POTLPT]2.0.CO;2.

Crittenden, M.D., Christie-Blick, N., Karl Link, P., 1983. Evidence for two pulses of glaciation during the late Proterozoic in northern Utah and southeastern Idaho. Geol. Soc. Am. Bull. 94, 437–450. https://doi.org/10.1130/0016-7606(1983)94<437:EFTPOG>2.0.CO;2.

Crittenden, M.D., Sharp, B.J., Calkins, F.C., 1952. Parleys Canyon to Traverse Range, in: Geology of the Wasatch Mountains East of Salt Lake City, Guidebook to the Geology of Utah. Utah Geological Association.

Crittenden, M.D., Wallace, C.A., 1973. Belt Symposium, Volume I | Idaho Geological Survey, in: Belt Symposium, Volume I. Idaho Geological Survey, Moscow, Idaho.

Crowell, John .C., 1957. Origin of Pebbly Mudstones. Geol Soc America Bull 68 (8), 993. https://doi.org/10.1130/0016-7606(1957)68[993:OOPM]2.0.CO;2.

Crowell, J.C., 1964. Climatic significance of sedimentary deposits containing dispersed megaclasts. In: Nairn, A.E.M. (Ed.), Problems in Palaeoclimatology. Interscience, London, pp. 86–99.

Daily, B., Gostin, V.A., Nelson, C.A., 1973. Tectonic origin for an assumed glacial pavement of Late Proterozoic age, South Australia. J. Geol. Soc. Aust. 20 (1), 75–78. https://doi.org/10.1080/14400957385270061.

Davies, B.J., 2008. British and Fennoscandian Ice-Sheet Interactions During the Quaternary (PhD Thesis). Durham University.
de Andrade Caxito, F., Halverson, G.P., Uhlein, A., Stevenson, R., Dias, T.G., Uhlein, G.J., 2012. Marinoan glaciation in east central Brazil. Precambr. Res. 200, 38–58. https://doi.org/10.1016/j.precamres.2012.01.005.
Dehler, C., Gehrels, G., Porter, S., Heizler, M., Karlstrom, K., Cox, G., Crossey, L., Timmons, M., 2017. Synthesis of the 780–740 Ma Chuar, Uinta Mountain, and Pahrump (ChUMP) groups, western USA: Implications for Laurentia-wide cratonic marine basins. Geol. Soc. Am. Bull. 129 (5-6), 607–624. https://doi.org/10.1130/B31532.110.1130/2016361.
Dehler, C.M., Fanning, C.M., Link, P.K., Kingsbury, E.M., Rybczynski, D., 2010. Maximum depositional age and provenance of the Uinta Mountain Group and Big Cottonwood Formation, northern Utah: Paleogeography of rifting western Laurentia. Geol. Soc. Am. Bull. 122 (9-10), 1686–1699. https://doi.org/10.1130/B30094.110.1130/2010129.
Dewez, T., Girardeau-Montaut, D., Allanic, C., Rohmer, J., 2016. Facets: A cloudcompare plugin to extract geological planes from unstructured 3d point clouds. 10.5194/isprsarchives-XLI-B5-799-2016.
Dey, S., Dasgupta, P., Das, K., Matin, A., 2020. Neoproterozoic Blaini Formation of Lesser Himalaya, India: Fiction and Fact. Geological Society of America bulletin. 10.1130/B35483.1.
Deynoux, M., 1985. Terrestrial or waterlain glacial diamictites? Three case studies from the Late Precambrian and Late Ordovician glacial drifts in West Africa. Palaeogeogr. Palaeoclimatol. Palaeoecol. 51 (1-4), 97–141. https://doi.org/10.1016/0031-0182(85)90082-3.
Ehlers, T.A., Chan, M.A., 1999. Tidal sedimentology and estuarine deposition of the proterozoic Big Cottonwood Formation. Utah. J. Sediment. Res. 69 (6), 1169–1180. https://doi.org/10.2110/jsr.69.1169.
Elison, M.W., Speed, R.C., Kistler, R.W., 1990. Geologic and isotopic constraints on the crustal structure of the northern Great Basin. GSA Bulletin 102, 1077–1092. https://doi.org/10.1130/0016-7606(1990)102<1077:GAICOT>2.3.CO;2.
Etemad-Saeed, N., Hosseini-Barzi, M., Adabi, M.H., Miller, N.R., Sadeghi, A., Houshmandzadeh, A., Stockli, D.F., 2016. Evidence for ca. 560 Ma Ediacaran glaciation in the Kahar Formation, central Alborz Mountains, northern Iran. Gondwana Res. 31, 164–183. https://doi.org/10.1016/j.gr.2015.01.005.
Etienne, J.L., Allen, P.A., Guerroué, E. le, Heaman, L., Ghosh, S.K., Islam, R., 2011. Chapter 31 The Blaini Formation of the Lesser Himalaya, NW India. Geological Society, London, Memoirs 36, 347–355. 10.1144/M36.31.
Eyles, N., Boyce, J.I., 1998. Kinematic indicators in fault gouge: tectonic analog for soft-bedded ice sheets. Sediment. Geol. 116 (1-2), 1–12. https://doi.org/10.1016/S0037-0738(97)00122-X.
Eyles, N., Januszczak, N., 2004. "Zipper-rift": a tectonic model for Neoproterozoic glaciations during the breakup of Rodinia after 750 Ma. Earth-Sci. Rev. 65 (1-2), 1–73. https://doi.org/10.1016/S0012-8252(03)00080-1.
Fanning, C.M., Link, P.K., 2004. U-Pb SHRIMP ages of Neoproterozoic (Sturtian) glaciogenic Pocatello Formation, southeastern Idaho. Geology 32 (10), 881. https://doi.org/10.1130/G20609.110.1130/2004146.
Gaschnig, R.M., Rudnick, R.L., McDonough, W.F., Kaufman, A.J., Valley, J.W., Hu, Z., Gao, S., Beck, M.L., 2016. Compositional evolution of the upper continental crust through time, as constrained by ancient glacial diamictites. Geochim. Cosmochim. Acta 186, 316–343. https://doi.org/10.1016/j.gca.2016.03.020.
Germs, G.J.B., 1972. Chapter V: Glacial Phenomena. In: Bulletin 12: The Stratigraphy and Paleontology of the Lower Nama Group South West Africa. Precambrian Research Unit, Department of Geology, University of Cape Town, Cape Town, South Africa, Chamber of Mines, pp. 97–107.
Germs, G.J.B., Gaucher, C., 2012. Nature and Extent of a Late Ediacaran (ca. 547 Ma) Glacigenic Erosion Surface in Southern Africa. S. Afr. J. Geol. 115 (1), 91–102. https://doi.org/10.2113/gssajg.115.91.
Gibling, M.R., 2006. Width and thickness of fluvial channel bodies and valley fills in the geological record: A literature compilation and classification. J. Sediment. Res. 76 (5), 731–770. https://doi.org/10.2110/jsr.2006.060.
Glasser, N.F., Bennett, M.R., 2004. Glacial erosional landforms: origins and significance for palaeoglaciology. Prog. Phys. Geogr. 28 (1), 43–75. https://doi.org/10.1191/0309133304pp401ra.
Grey, K., Corkeron, M., 1998. Late Neoproterozoic stromatolites in glacigenic successions of the Kimberley region, Western Australia: Evidence for a younger Marinoan glaciation. Precambrian Res. 92, 65–87. https://doi.org/10.1016/S0301-9268(98)00068-0.
Hambrey, M.J., Glasser, N.F., 2012. Discriminating glacier thermal and dynamic regimes in the sedimentary record. Sediment. Geol. 251, 1–33. https://doi.org/10.1016/j.sedgeo.2012.01.008.
Hancock, G.S., Anderson, R.S., Whipple, K.X., 1998. Beyond Power: Bedrock River Incision Process and Form. https://doi.org/10.1029/GM107p0035.
Hicock, S.R., Goff, J.R., Lian, O.B., Little, E.C., 1996. On the interpretation of subglacial till fabric. J. Sediment. Res. 66, 928–934. https://doi.org/10.1306/D4268441-2B26-11D7-8648000102C1865D.
Hintze, F.F., 1914. A Contribution to the Geology of the Wasatch Mountains, Utah. Annals of the New York Academy of Sciences 23, 85–143. 10.1111/j.1749-6632.1914.tb56939.x.
Hoffman, P.F., Abbot, D.S., Ashkenazy, Y., Benn, D.I., Brocks, J.J., Cohen, P.A., Cox, G. M., Creveling, J.R., Donnadieu, Y., Erwin, D.H., Fairchild, I.J., Ferreira, D., Goodman, J.C., Halverson, G.P., Jansen, M.F., Le Hir, G., Love, G.D., Macdonald, F. A., Maloof, A.C., Partin, C.A., Ramstein, G., Rose, B.E.J., Rose, C.V., Sadler, P.M., Tziperman, E., Voigt, A., Warren, S.G., 2017. Snowball Earth climate dynamics and Cryogenian geology-geobiology. Sci. Adv. 3 (11), e1600983. https://doi.org/10.1126/sciadv.1600983.
Hoffman, P.F., Kaufman, A.J., Halverson, G.P., Schrag, D.P., 1998. A Neoproterozoic snowball earth. Science 281, 1342–1346. https://doi.org/10.1126/science.281.5381.1342.
Isotta, Carlos A.L., Rocha-Campos, A.C., Yoshida, R., 1969. Striated Pavement of the Upper Pre-Cambrian Glaciation in Brazil. Nature 222 (5192), 466–468. https://doi.org/10.1038/222466a0.
Jensen, P.A., Wulff-Pedersen, E., 1996. Glacial or non-glacial origin for the Bigganjargga tillite, Finnmark, Northern Norway. Geol. Mag. 133 (2), 137–145. https://doi.org/10.1017/S0016756800008657.
Johnston, S.T., 2008. The Cordilleran Ribbon Continent of North America. Annu. Rev. Earth Planet. Sci. 36 (1), 495–530. https://doi.org/10.1146/annurev.earth.36.031207.124331.
Karlstrom, K.E., Bowring, S.A., Dehler, C.M., Knoll, A.H., Porter, S.M., Marais, D.J.D., Weil, A.B., Sharp, Z.D., Geissman, J.W., Elrick, M.B., Timmons, J.M., Crossey, L.J., Davidek, K.L., 2000. Chuar Group of the Grand Canyon: Record of breakup of Rodinia, associated change in the global carbon cycle, and ecosystem expansion by 740 Ma. Geology 28, 619–622. https://doi.org/10.1130/0091-7613(2000)28<619:CGOTGC>2.0.CO;2.
Keeley, J.A., Link, P.K., Fanning, C.M., Schmitz, M.D., 2013. Pre- to synglacial rift-related volcanism in the Neoproterozoic (Cryogenian) Pocatello Formation, SE Idaho: New SHRIMP and CA-ID-TIMS constraints. Lithosphere 5, 128–150. 10.1130/L226.1.
Kellerhals, P., Matter, A., 2003. Facies analysis of a glaciomarine sequence, the Neotproterozoic Mirbat Sandstone Formation, Sultanate of Oman. Eclogae Geol. Helv. 96, 49–70. https://doi.org/10.1007/S00015-003-1068-3.
Kennedy, K., Eyles, N., 2020. Syn-rift mass flow generated 'tectonofacies' and 'tectonosequences' of the Kingston Peak Formation, Death Valley, California, and their bearing on supposed Neoproterozoic panglacial climates. Sedimentology 68, 352–381. 10.1111/sed.12781.
King, E.L., Haflidason, H., Sejrup, H.P., Løvlie, R., 1998. Glacigenic debris flows on the North Sea Trough Mouth Fan during ice stream maxima. Mar. Geol. 152 (1-3), 217–246. https://doi.org/10.1016/S0025-3227(98)00072-3.
Kirschvink, J.L., 1992. Late Proterozoic low-latitude global glaciation: the snowball Earth. In: Schopf, J.W., Klein, C., Des Maris, D. (Eds.), The Proterozoic Biosphere: A Multidisciplinary Study. Cambridge University Press, pp. 51–52.
Kumpulainen, R.A., Greiling, R.O., 2011. Chapter 60 Evidence for late Neoproterozoic glaciation in the central Scandinavian Caledonides. Geological Society, London, Memoirs 36, 623–628. 10.1144/M36.60.
Laajoki, K., 2002. New evidence of glacial abrasion of the Late Proterozoic unconformity around Varangerfjorden, northern Norway. In: Altermann, W., Corcoran, P.L. (Eds.), Precambrian Sedimentary Environments: A Modern Approach to Ancient Depositional Systems. Special Publication of International Association of Sedimmentologists, Blackwell Science, pp. 405–436.
Le Heron, D.P., 2018. An exhumed Paleozoic glacial landscape in Chad. Geology 46, 91–94. https://doi.org/10.1130/G39510.1.
Le Heron, D.P., Eyles, N., Busfield, M.E., 2020. The Laurentian Neoproterozoic Glacial Interval: Reappraising the extent and timing of glaciation. Journal of Austrian Earth Sciences. 10.17738/ajes.2020.0004.
Le Heron, D.P., Vandyk, T.M., Kuang, H., Liu, Y., Chen, X., Wang, Y., Yang, Z., Sharfenberg, L., Davies, B., Shields-Zhou, G., 2019. A bird's eye view of an Ediacaran subglacial landscape. Geology. 10.1130/G46285.1.
Le Heron, D.P., Vandyk, T.M., Wu, G., Li, M., 2018. New perspectives on the Luoquan Glaciation (Ediacaran-Cambrian) of North China. The Depositional Record 4 (2), 274–292. https://doi.org/10.1002/dep2.2018.4.issue-210.1002/dep2.46.
Lechte, M.A., Wallace, M.W., van Hood, A., S., Planavsky, N.,, 2018. Cryogenian iron formations in the glaciogenic Kingston Peak Formation. California. Precambrian Res. 310, 443–462. https://doi.org/10.1016/j.precamres.2018.04.003.
Levy, M., Christie-Blick, N., 1991. Late Proterozoic Paleogeography of the Eastern Great Basin 371–386.
Levy, M., Christie-Blick, N., 1989. Pre-Mesozoic palinspastic reconstruction of the eastern Great Basin (western United States). Science 245 (4925), 1454–1462. https://doi.org/10.1126/science:245.4925.1454.
Levy, M., Christie-Blick, N., Link, P.K., 1994. Neoproterozoic incised valleys of the eastern Great Basin, Utah and Idaho: Fluvial response to changes in depositional base level. in: SEPM Special Publication 51: Incised Valley Systems: Origin and Sedimentary Sequences. Society for Sedimentary Geology (SEPM).
Link, P.K., Christie-Blick, N., 2011. Chapter 38 Neoproterozoic strata of southeastern Idaho and Utah: record of Cryogenian rifting and glaciation. Geological Society, London, Memoirs 36, 425–436. 10.1144/M36.38.
Lund, K., 2008. Geometry of the Neoproterozoic and Paleozoic rift margin of western Laurentia: Implications for mineral deposit settings. Geosphere 4, 429–444. https://doi.org/10.1130/GES00121.1.
Macdonald, F.A., Prave, A.R., Petterson, R., Smith, E.F., Pruss, S.B., Oates, K., Waechter, F., Trotzuk, D., Fallick, A.E., 2013. The Laurentian record of Neoproterozoic glaciation, tectonism, and eukaryotic evolution in Death Valley, California. Geol. Soc. Am. Bull. 125 (7-8), 1203–1223. https://doi.org/10.1130/B30789.110.1130/2013253.
Mckee, E., Weir, G., 1953. Terminology for Stratification and Cross-Stratification in Sedimentary Rocks. Geol. Soc. Am. Bull. 64, 381–390. https://doi.org/10.1130/0016-7606(1953)64[381:TFSACI]2.0.CO;2.
Metashape, 2020. Agisoft. Version 1.6.2 Build 10247. https://www.agisoft.com/.
Miller, Jerry R., 1991. The Influence of Bedrock Geology on Knickpoint Development and Channel-Bed Degradation Along Downcutting Streams in South-Central Indiana. J. Geol. 99 (4), 591–605. https://doi.org/10.1086/629519.
Moncrieff, A.C.M., Hambrey, M.J., 1988. Late Precambrian Glacially-Related Grooved and Striated Surfaces in the Tillite Group of Central East Greenland. Paleogeogr.

Paleoclimatol. Paleoecol. 65 (3-4), 183–200. https://doi.org/10.1016/0031-0182(88)90023-5.
Montes, A.S.L., Gravenor, C.P., Montes, M.L., 1985. Glacial sedimentation in the late Precambrian Bebedouro formation, Bahia, Brazil. Sediment. Geol. 44 (3-4), 349–358. https://doi.org/10.1016/0037-0738(85)90019-3.
Moynihan, D.P., Strauss, J., Nelson, L.L., Padget, C.D., 2019. Upper Windermere Supergroup and the transition from rifting to continent-margin sedimentation, Nadaleen River area, northern Canadian Cordillera. Geol. Soc. Am. Bull. 131, 1673–1701. https://doi.org/10.1130/B32039.1.
Nystuen, Johan P., Lamminen, Jarkko T., 2011. Neoproterozoic glaciation of South Norway: from continental interior to rift and pericratonic basins in western Baltica. Geological Society, London, Memoirs 36, 613–622. https://doi.org/10.1144/M36.59.
Ojakangas, R., Matsch, C., 1980. Upper Precambrian (eocambrian) Mineral Fork Tillite of Utah - a Continental Glacial and Glaciomarine Sequence. Geol. Soc. Am. Bull. 91, 495–501. https://doi.org/10.1130/0016-7606(1980)91<495:UPEMFT>2.0.CO;2.
Pang, G., Koper, K.D., Mesimeri, M., Pankow, K.L., Baker, B., Farrell, J., Holt, J., Hale, J. M., Roberson, P., Burlacu, R., Pechmann, J.C., Whidden, K., Holt, M.M., Allam, A., DuRoss, C., 2020. Seismic Analysis of the 2020 Magna, Utah, Earthquake Sequence: Evidence for a Listric Wasatch Fault. Geophysical Research Letters 47, e2020GL089798. 10.1029/2020GL089798.
Paulsen, Timothy, Marshak, Stephen, 1999. Origin of the Uinta recess, Sevier fold–thrust belt, Utah: influence of basin architecture on fold–thrust belt geometry. Tectonophysics 312 (2-4), 203–216. https://doi.org/10.1016/S0040-1951(99)00182-1.
Perry, W.J., Roberts, H.G., 1968. Late Precambrian glaciated pavements in the Kimberley region, Western Australia. J. Geol. Soc. Aust. 15 (1), 51–56. https://doi.org/10.1080/00167616808728679.
Preiss, W.V., Gostin, V.A., McKirdy, D.M., Ashley, P.M., Williams, G.E., Schmidt, P.W., 2011. Chapter 69 The glacial succession of Sturtian age in South Australia: the Yudnamutana Subgroup. Geological Society, London, Memoirs 36, 701–712. 10.1144/M36.69.
Quirk, B.J., Moore, J.R., Laabs, B.J.C., Caffee, M.W., Plummer, M.A., 2018. Termination II, Last Glacial Maximum, and Lateglacial chronologies and paleoclimate from Big Cottonwood Canyon, Wasatch Mountains. Utah. Geol. Soc. Am. Bull. 130, 1889–1902. https://doi.org/10.1130/B31967.1.
Rice, A.H.N., Edwards, M.B., Hansen, T.A., Arnaud, E., Halverson, G.P., 2011. Chapter 57 Glaciogenic rocks of the Neoproterozoic Smalfjord and Mortensnes formations, Vestertana Group, E. Finnmark, Norway. Geological Society, London, Memoirs 36, 593–602. 10.1144/M36.57.
Richardson, K., Carling, P.A., 2005. Typology of Sculpted Forms in Open Bedrock Channels, in: Typology of Sculpted Forms in Open Bedrock Channels. Geological Soc Amer Inc, Boulder, pp. 1–108. 10.1130/2005.2392-2.1.
Rice, A.H.N., Hofmann, C.-C., 2000. Evidence for a glacial origin of Neoproterozoic III striations at Oaibaˇcˇannjar'ga, Finnmark, northern Norway. Geol. Mag. 137 (4), 355–366. https://doi.org/10.1017/S0016756800004222.
Rieu, R., Allen, P.A., Etienne, J.L., Cozzi, A., Wiechert, U., 2006. A Neoproterozoic glacially influenced basin margin succession and "atypical" cap carbonate associated with bedrock palaeovalleys, Mirbat area, southern Oman. Basin Res. 18, 471–496. https://doi.org/10.1111/j.1365-2117.2006.00304.x.
Rose, Brian E.J., 2015. Stable "Waterbelt" climates controlled by tropical ocean heat transport: A nonlinear coupled climate mechanism of relevance to Snowball Earth. J. Geophys. Res.-Atmos. 120 (4), 1404–1423. https://doi.org/10.1002/2014JD022659.
Scott, D.N., Wohl, E.E., 2019. Bedrock fracture influences on geomorphic process and form across process domains and scales. Earth Surf. Proc. Land. 44, 27–45. https://doi.org/10.1002/esp.4473.
Shaw, J., Gilbert, R.G., Sharpe, D.R., Lesemann, J.-E., Young, R.R., 2020. The origins of s-forms: Form similarity, process analogy, and links to high-energy, subglacial meltwater flows. Earth-Sci. Rev. 200, UNSP 102994. 10.1016/j.earscirev.2019.102994.
Shields-Zhou, G.A., Deynoux, M., Och, L., 2011. Chapter 11 The record of Neoproterozoic glaciation in the Taoudéni Basin, NW Africa. Geological Society, London, Memoirs 36, 163–171. 10.1144/M36.11.
Siman-Tov, S., Stock, G.M., Brodsky, E.E., White, J.C., 2017. The coating layer of glacial polish. Geology 45, 987–990. https://doi.org/10.1130/G39281.1.
Southwick, D.L., Morey, G.B., Mossler, J.H., 1986. Fluvial origin of the lower Proterozoic Sioux Quartzite, southwestern Minnesota. GSA Bulletin 97, 1432–1441. https://doi.org/10.1130/0016-7606(1986)97<1432:FOOTLP>2.0.CO;2.
Spence, G.H., Le Heron, D.P., Fairchild, I.J., 2016. Sedimentological perspectives on climatic, atmospheric and environmental change in the Neoproterozoic Era. Sedimentology. https://doi.org/10.1111/sed.12261.
Spencer, C.J., Hoiland, C.W., Harris, R.A., Link, P.K., Balgord, E.A., 2012. Constraining the timing and provenance of the Neoproterozoic Little Willow and Big Cottonwood Formations, Utah: Expanding the sedimentary record for early rifting of Rodinia. Precambrian Res. 204, 57–65. https://doi.org/10.1016/j.precamres.2012.02.009.
State of Utah, 2012. High Resolution Orthophotography (HRO) 6-inch (12.5 cm) resolution 4-band aerial photography from 2012 for the Wasatch Front. Available at https://gis.utah.gov/data/aerial-photography/hro/.
State of Utah, 2006. 2 meter Bare Earth DEMs for Wasatch Front, Heber and Iron County areas (LIDAR). Available at https://gis.utah.gov/data/elevation-and-terrain/2-meter-lidar/.
Stock, G.M., Frankel, K.L., Ehlers, T.A., Schaller, M., Briggs, S.M., Finkel, R.C., 2009. Spatial and temporal variations in denudation of the Wasatch Mountains, Utah, USA. Lithosphere 1, 34–40. https://doi.org/10.1130/L15.1.
Stouge, S., Christiansen, J.L., Harper, D.A.T., Houmark-Nielsen, M., Kristiansen, K., MacNiocaill, C., Buchardt-Westergård, B., 2011. Chapter 56 Neoproterozoic (Cryogenian–Ediacaran) deposits in East and North-East Greenland. Geological Society, London, Memoirs 36, 581–592. 10.1144/M36.56.
Talley, L.D., Pickard, G.L., Emery, W.J., Swift, J.H., 2011. Chapter 13 - Southern Ocean. In: Talley, L.D., Pickard, G.L., Emery, W.J., Swift, J.H. (Eds.), Descriptive Physical Oceanography (Sixth Edition). Academic Press, Boston, pp. 437–471. https://doi.org/10.1016/B978-0-7506-4552-2.10013-7.
Thiele, S.T., Grose, L., Samsu, A., Micklethwaite, S., Vollgger, S.A., Cruden, A.R., 2017. Rapid, semi-automatic fracture and contact mapping for point clouds, images and geophysical data. Solid Earth 8, 1241. https://doi.org/10.5194/se-8-1241-2017.
Trosdtorf, I., Rocha-Campos, A.C., dos Santos, P.R., Tomio, A., 2005. Origin of Late Paleozoic, multiple, glacially striated surfaces in northern Parana Basin (Brazil): Some implications for the dynamics of the Parana glacial lobe. Sediment. Geol. 181, 59–71. https://doi.org/10.1016/j.sedgeo.2005.07.006.
van Loon, A.J., 2008. Could 'Snowball Earth' have left thick glaciomarine deposits? Gondwana Research, Snowball Earth to Cambrian Explosion 14, 73–81. https://doi.org/10.1016/j.gr.2007.05.009.
Vandyk, T.M., Wu, G., Davies, B., Xiao, Y., Li, M., Shields-Zhou, G., le Heron, D., 2019. Temperate glaciation on a Snowball Earth: Glaciological and palaeogeographic insights from the Cryogenian Yuermeinak Formation of NW China. Precambr. Res. https://doi.org/10.1016/j.precamres.2019.105362.
Varney, P.J., 1976. Depositional Environment of the Mineral Fork Formation (Precambrian), Wasatch Mountains, Utah, in: Geology of the Cordilleran Hingeline: Rocky Mountain Association of Geologists Symposium. Rocky Mountain Association of Geologists, pp. 91–102.
Vernhet, E., Youbi, N., Chellai, E.H., Villeneuve, M., El Archi, A., 2012. The Bou-Azzer glaciation: Evidence for an Ediacaran glaciation on the West African Craton (Anti-Atlas, Morocco). Precambrian Res. 196, 106–112. https://doi.org/10.1016/j.precamres.2011.11.009.
Weil, A.B., Geissman, J.W., Ashby, J.M., 2006. A new paleomagnetic pole for the Neoproterozoic Uinta Mountain supergroup, Central Rocky Mountain States, USA. Precambrian Res. 147, 234–259. https://doi.org/10.1016/j.precamres.2006.01.017.
Wilken, M., Mienert, J., 2006. Submarine glacigenic debris flows, deep-sea channels and past ice-stream behaviour of the East Greenland continental margin. Quat. Sci. Rev. 25, 784–810. https://doi.org/10.1016/j.quascirev.2005.06.004.
Wray, R.A.L., Sauro, F., 2017. An updated global review of solutional weathering processes and forms in quartz sandstones and quartzites. Earth-Sci. Rev. 171, 520–557. https://doi.org/10.1016/j.earscirev.2017.06.008.
Xue, L., Gani, N.D., Abdelsalam, M.G., 2019. Drainage incision, tectonic uplift, magmatic activity, and paleo-environmental changes in the Kenya Rift, East African Rift System: A morpho-tectonic analysis. Geomorphology 345, 106839. https://doi.org/10.1016/j.geomorph.2019.106839.
Yonkee, W.A., Dehler, C.D., Link, P.K., Balgord, E.A., Keeley, J.A., Hayes, D.S., Wells, M. L., Fanning, C.M., Johnston, S.M., 2014. Tectono-stratigraphic framework of Neoproterozoic to Cambrian strata, west-central US: Protracted rifting, glaciation, and evolution of the North American Cordilleran margin. Earth Sci. Rev. 136, 59–95. https://doi.org/10.1016/j.earscirev.2014.05.004.
Yonkee, W.A., Weil, A.B., 2015. Tectonic evolution of the Sevier and Laramide belts within the North American Cordillera orogenic system. Earth-Sci. Rev. 150, 531–593. https://doi.org/10.1016/j.earscirev.2015.08.001.
Young, G.M., 2002. Geochemical investigation of a Neoproterozoic glacial unit: the Mineral Fork Formation in the Wasatch Range, Utah. Geol. Soc. Am. Bull. 114, 387–399.
Young, R.W., Wray, R.A.L., Young, A.R.M., 2009. Chapter 2: Variations within sandstones. Sandstone Landforms. Cambridge University Press.
Ziegler, M., Loew, S., Bahat, D., 2014. Growth of exfoliation joints and near-surface stress orientations inferred from fractographic markings observed in the upper Aar valley (Swiss Alps). Tectonophysics 626, 1–20. https://doi.org/10.1016/j.tecto.2014.03.017.